# INVESTIGATION OF THE NEURAL BASIS OF NATURAL ACTION PERCEPTION WITHIN THE THEORETICAL FRAMEWORK OF PERCEPTUAL DECISION MAKING

A THESIS SUBMITTED TO

THE GRADUATE SCHOOL OF ENGINEERING AND SCIENCE

OF BILKENT UNIVERSITY

IN PARTIAL FULFILLMENT OF THE REQUIREMENTS FOR

THE DEGREE OF

MASTER OF SCIENCE

IN

NEUROSCIENCE

By

Şeyda EVSEN

July 2024

Investigation of the Neural Basis of Natural Action Perception within the Theoretical Framework of Perceptual Decision Making
By Şeyda EVSEN
July 2024

We certify that we have read this thesis and that in our opinion it is fully adequate, in scope and in quality, as a thesis for the degree of Master of Science.

Burcu Ayşen ÜRGEN(Advisor)

Zahide PAMİR KARATOK

Didem KADIHASANOĞLU

Approved for the Graduate School of Engineering and Science:

Orhan ARIKAN
Director of the Graduate School

# ABSTRACT

# INVESTIGATION OF THE NEURAL BASIS OF NATURAL ACTION PERCEPTION WITHIN THE THEORETICAL FRAMEWORK OF PERCEPTUAL DECISION MAKING

Şeyda EVSEN
M.S. in Neuroscience
Advisor: Burcu Ayşen ÜRGEN
July 2024

Every day, we perceive many actions performed by people around us. Understanding the movements we perceive and the intentions behind these movements is critical to determining how to respond to the observed action. Neurophysiology studies and computational model theories suggest that this perceptual decision process consists of two stages: accumulation of encoded sensory evidence and selection of response. EEG studies in humans have identified a neural trace thought to represent the first of these two stages: Centro Parietal Positivity (CPP), which scales with the strength of the incoming sensory evidence and differs from the Lateralized Readiness Potential (LRP) that represents motor preparatory activity. However, these studies mainly utilized simple and artificial stimuli; therefore, whether perceptual decision-making processes will be similar when processing a more complex and ecologically meaningful stimulus, such as natural actions, is an open question. This study aimed to investigate this gap in the literature by examining the neural basis of perceptual decisions related to the perception of natural actions.

To this end, in this study, which included three separate EEG sessions, twenty participants performed a discrimination task between action exemplars belonging to a different action class in each session (either one of the locomotion, skin-displacement actions, or manipulation actions). To control for task difficulty, the same coherence manipulation was applied to each action exemplar to create four levels of coherence, and behavioral data analysis showed that mean response times and miss rates decreased as the level of coherence increased.

Furthermore, the results of event-related potential analysis showed that the CPP signal followed the level of coherence of the stimulus within all action classes, which is in line with the literature, and also that the manipulation of the action class had a significant effect on the CPP signal. In contrast to CPP, the LRP signal showed an independent build-up from both the strength of the sensory evidence and the identity of the action class.

Taken together, the findings of the current study support the generalizability of perceptual decision-making stages and their neural basis, which are defined by utilizing much simpler stimuli, to decisions related to the perception of natural actions while revealing that the identity of natural movements significantly influences the decision process.

*Keywords:* Perceptual Decision Making, Natural Action Perception, Centro Parietal Positivity.

# ÖZET

# DOĞAL EYLEM ALGISININ NÖRAL TEMELLERİNİN ALGISAL KARAR VERME TEORİK ÇERÇEVESİNDE İNCELENMESİ

Şeyda EVSEN
Sinirbilim, Yüksek Lisans
Tez Danışmanı: Burcu Ayşen ÜRGEN
Temmuz 2024

Her gün, etrafımızdaki insanlar tarafından gerçekleştirilen pek çok eylem algılarız. Algıladığımız bu hareketleri ve bu hareketlerin arkasındaki niyetleri anlamak, gözlemlenen eyleme oluşturulacak cevaba karar verilmesi için kritiktir. Nörofizyoloji çalışmaları ve hesaplamalı model teorileri, bu algısal karar sürecinin iki aşamadan oluştuğunu ileri sürmektedir: kodlanmış duyusal kanıtların birikmesi ve yanıt seçimi. İnsanlarda yapılan EEG çalışmaları, bu iki aşamadan ilkini temsil ettiği düşünülen nöral bir iz tespit etmiştir: Gelen duyusal kanıtların gücüyle ölçeklenen ve motor hazırlığını temsil eden Lateralized Readiness Potansiyeli'nden (LRP) farklı olan Centro Parietal Pozitifliği (CPP). Ancak bu çalışmalarda çoğunlukla basit ve yapay uyaranlar kullanılmıştır; dolayısıyla doğal eylemler gibi daha karmaşık ve ekolojik açıdan anlamlı bir uyaranı işlerken algısal karar alma süreçlerinin benzer olup olmayacağı açık bir sorudur. Bu çalışma, doğal eylemlerin algılanmasıyla ilgili algısal kararların sinirsel temelini inceleyerek literatürdeki bu boşluğu araştırmayı amaçlamıştır.

Bu amaçla, üç ayrı EEG oturumu içeren bu çalışmada, yirmi katılımcı her oturumda farklı bir eylem sınıfına ait (hareket eylemleri, kişinin kendine yönelik hareketleri veya manipülasyon eylem sınıflarından biri) eylem örnekleri arasında bir ayrıştırma görevi gerçekleştirmiştir. Görev zorluğunu kontrol etmek için her bir eylem örneği üzerinde aynı uyumluluk manipülasyonu uygulanarak dört uyumluluk seviyesi oluşturulmuştur; davranışsal veri analizi ise uyumluluk seviyesinin artmasıyla birlikte ortalama yanıt sürelerinin ve kaçırma oranlarının azaldığını göstermiştir.

Bununla birlikte, olaya-ilişkin potansiyel analizi sonuçları CPP sinyalinin tüm eylem sınıfları içerisinde -literatürle uygun olarak- uyaranın uyumluluk seviyesini

takip ettiğini ve aynı zamanda eylem sınıfı manipülasyonunun CPP sinyali üzerinde önemli bir etkisi olduğunu göstermiştir. CPP'nin aksine, LRP sinyali hem duyusal kanıtın gücünden hem de eylem sınıfının kimliğinden bağımsız bir oluşum sergilemiştir.

Mevcut çalışmanın bulguları bir arada değerlendirildiğinde, çok daha basit uyaranların kullanılmasıyla tanımlanmış algısal karar verme aşamalarının ve bu aşamaların sinirsel temellerinin doğal eylemlerin algılanmasını içeren kararlara genellenebilirliğini desteklerken, doğal hareketlerin kimliğinin karar sürecini önemli ölçüde etkilediğini ortaya koymaktadır.

*Anahtar sözcükler*: Algısal Karar Verme, Doğal Hareket Algısı, Centro Parietal Positivite.

# Acknowledgement

First and foremost, I would like to express my gratitude to my advisor, Dr. Burcu Ayşen Ürgen, for her endless support and faith in me throughout my master's journey. Without her encouragement and guidance, this thesis would not have reached its current form. Furthermore, I would like to thank my thesis committee members, Dr. Zahide Pamir Karatok and Dr. Didem Kadıhasanoğlu, for their valuable time and comments.

I would like to thank the Health Institutes of Türkiye (TÜSEB) for their financial support during my master's studies under the TÜSEB-B grant with project number 27732.

I am deeply grateful to my family: my mother, Zekiye Evsen, who taught me to be resilient and has been the wind beneath my arms; my father, Bahittin Evsen, who has been a mentor and a dim of sunshine with his endless positive attitude; and my sister, Setenay Evsen, who has been my role model and considerate critic. I am sincerely thankful for their unconditional support and efforts in helping me chase my career goals. At times of self-doubt, they have become my strength and motivation. I also wish to thank and express my sincere gratitude to my best friend, Nursena Bölük, for her limitless support and for being the best "best friend" I could ever ask for; and to Batuhan Balcıoğlu, for giving me the courage to pursue my goals, being my partner in my struggles, and supporting me in my decisions.

Also, I would like to thank Dr. Faruk Takaoğlu for his interest in my research, for being ready to help, and for supporting me throughout my master's education.

Furthermore, I am thankful to my dearest friends from Aysel Sabuncu Brain Research Center, Berrak Müftüoğlu, Sezan Mert, Aslı Eroğlu, Rabia Nur Kılıç, Tuğçe Nur Pekçetin, Gaye Aşkın, and Tuvana Karaduman for making graduate life much more enjoyable.

Last but not least, I would like to thank the members of the Cognitive Computational Neuroscience Lab and our undergraduate EEG research assistants, Ömer Rençbereli, Badel Barinal, Ayaz Karadağ, Cenk Günsel, Ataol Burak Özsu, Can Atasayar, Melis Akdeniz, Melissa Nur Robinson, Nurbanu Çakır, Harun Olur for their effort and contributions in data collection.

# Contents

# List of Figures

# List of Tables

# Chapter 1

# Introduction

Perceiving and understanding the actions of conspecifics and other animals is an important function of the human brain. The successful execution of this function is vital for the survival of both the perceived and the perceiver since many of the daily decisions are made based on the perceived sensory information. If anything goes wrong in the perception stage, the following decision process will be affected by it. For example, consider a person driving a car who fails to detect a pedestrian running to cross the street. In this scenario, it is highly likely that the driver will decide not to stop the car, hence creating a life-threatening condition for the pedestrian.

Despite having such an important place in daily life decisions, the number of studies investigating the perception of human actions within the framework of perceptual decision-making processes is scarce. Accordingly, this study targeted this gap in the literature and aimed to investigate the perceptual decision-making processes involved in the perception of actions of humans, as well as the neurophysiological basis of these processes, through a series of action discrimination tasks.

In what follows, I will review the important findings from the perceptual decision-making literature which shaped the current study. Then, I will briefly

discuss the findings on the neural basis of biological motion perception. Finally, I will discuss two studies that are essential in our understanding of discrimination of observed natural actions.

## 1.1 Perceptual Decision Making

Decision-making, simply defined as the act of choosing one option from several alternatives, is an essential part of everyday life. Throughout the day, people constantly make decisions with differing purposes, and these purposes change the cognitive level at which the decisions are made. The decisions that are made at a lower cognitive level include decisions that have one true value (there is an objectively correct option between the alternatives). These decisions are generally made in short time intervals, such as judging whether the traffic light is green or red to push the brakes of the car, and they are defined as *perceptual decisions* [1]. On the contrary, the decisions that are made at a higher cognitive level generally require more deliberation and don't necessarily have a true value since they depend on the subjective goals of the deciding agent, such as deciding to enter the stock market, these classes of decisions are defined as *preferential decisions* [2]. The fast and objective nature of the perceptual decisions makes them valuable processes that can be regarded as test-benches for the investigation of the intermediate stage between sensation and action, *the stage where decision formation occurs*.

### 1.1.1 Computational Accounts of Perceptual Decisions

Perceptual decisions have been largely studied through 2-alternative-forced choice tasks (2AFCs), where the decision maker must commit to one of the alternatives. Following the work of Donders [3], much of the data obtained from behavioral experiments on perceptual judgments were inspected mainly through the response times (RTs). However, this approach has been challenged due to its core assumption that the identification of stimulus information and the response selection are

considered to be completed before the response execution [4]. An alternative to this approach has come from sequential sampling models(SSMs) of mathematical psychology. A particularly favored branch of SSMs is the standard diffusion model (or the drift-diffusion model (DDM)), which defines the decision process as the sequential accumulation of noisy sensory information into a decision variable (DV) that scales with the amount of sensory evidence and triggers a response at the instant it reaches one of the bounds [5]. The formulation of DDM enables it to explain the accuracy, the mean values, and the distributions of RTs separately for correct and incorrect trials [5] where the RT as a quantity comprised of two components as decision time and a non-decision time.

A decision process is defined over four main parameters in the framework of DDM: (i) bounds or boundary separation, representing the amount of cumulative evidence required to initiate a response; (ii) starting point, corresponding to the initial point from where the accumulation begins, (iii) drift rate, $v$, defining the speed of evidence accumulation, and (iv) non-decision time, encapsulating the time elapses while the encoding of stimulus and the time to execute to motor response [1, 5, 6, 7, 8].

A DDM approach for explaining behavioral data has the advantage of inferring information for the latent cognitive processes that are difficult to track solely on the mean RTs. DDM's parameters have been found to be associated with cognitive processes underlying the choice behavior. The boundary separation parameter is shown to be linked to the speed-accuracy trade-off (i.e., the implicit tendency or external manipulation of the experimenter that leads the decision-maker to prioritize either responding fast or correctly) with higher values of bound corresponding to emphasis on being accurate and lower values corresponding to emphasis on being fast [9]. The drift rate is found to be highly impacted by the strength of sensory evidence and the task difficulty; as the strength of the sensory evidence or the easiness of the task increases, higher drift rate values have been observed [5]. Biases towards one of either alternative mainly appear to be affecting the starting point of the accumulation process; if one of the alternatives is more appealing or more likely to be accurate/beneficial, the starting point deviates from the non-biased location towards the biased option [5, 10].

### 1.1.2 Neural Basis of Perceptual Decision-Making

The neural basis of perceptual decision-making has been extensively studied in rodents, primates, and humans using different tasks [11, 12]. In studying visual perceptual decisions, one of the most established paradigms is the discrimination of the net movement direction of randomly moving dots in a cloud (also known as the Random-Dot-Motion (RDM) Paradigm). The task difficulty, usually assessed with a parameter called as **coherence**, is achieved by manipulating the percentage of the coherently moving dots, assuming the task is to judge whether the net movement is towards direction $A$ or $B$, 50% coherence means that half of the dots in the visual stimuli is headed towards the same direction (say, direction A) while the rest of the dots are directing to random directions. In a similar manner, 100% coherence means that all the dots are moving in the same direction. In this framework, the coherently moving dots are referred to as motion signals, whereas incoherently moving dots are referred to as noise dots [13]. Coherence manipulation is favored because it enables the injection of noise into the decision process in a controlled manner, thus easing the investigation of stages of decision-making.

The RDM paradigm has been widely implemented in non-human primate neurophysiology studies as the paradigm is suitable for investigating the intermediate stage, which is hypothesized to be representative of decision formation, between the encoding of sensory stimulus and behavioral response execution [14, 15, 16, 17, 18]. Previous monkey studies have established areas MT/V5 and MST in the extrastriate cortex as the locations housing motion-selective neurons that respond according to their preferred direction [13, 19, 20], while the superior colliculus (SC) [21] and frontal eye field (FEF)[22] have been found to have critical roles in the generation of motor signals that would yield to saccadic eye movements. The lateral intraparietal area (LIP) of the posterior parietal cortex (PPC), which receives inputs from sensory encoding areas (MT and MST) and projects to motor areas (SC and FEF), has been investigated as a candidate location to probe a neural signature of decision formation [14].

These studies observed that the neurons in the LIP started eliciting signals

showing build-ups early in the stimulus presentation period [15, 16] and held their activity level until the response was executed [15]. The former outcome has been considered a neural trace of sequential accumulation of the sensory information on the net motion direction (*the net motion direction* refers to the difference between the firings of the two neuron populations selective to opposite directions). The latter was seen as a feature that distinguished the signal of interest from a purely sensory origin, as the responses evoked due to stimulus properties have been observed to diminish as the stimulus is removed from the visual field. Another important observation was related to the speed of evidence accumulation; as the coherence of the stimulus increased, the observed build-up rate in the responses was found to increase. The existence of such a dependency on the stimulus strength has been interpreted as the elimination of the possibility that the signal was a purely motor origin since a motor signal should not *directly* depend on the representations of the stimuli. These outcomes have strengthened the candidacy of LIP to be involved in the formation of a decision variable by temporally integrating the relevant sensory representations.

Inspired by the non-human primate neurophysiology findings, which indicated a temporal integration of the difference of sensory representations for two alternatives, over the last decades, researchers developed new paradigms to investigate whether a similar chain of computations was operating in the human brain by using different approaches: imaging (functional magnetic resonance imaging (fMRI)) [12] and neurophysiology (electroencephalography (EEG) and magnetoencephalography (MEG)) [23, 24, 25].

In order to find a neural signature that is representative of the decision process, O'Connell, Dockree, and Kelly [26] have designed a series of gradual detection tasks where they manipulated a specific feature of the stimuli (contrast for visual task, frequency or loudness for auditory task) with or without an overtly motor response and recorded the scalp EEG of participants. The gradual presentation of the stimulus has eliminated the sensory evoked visual potentials (SSVEPs) from the time course of event-related potentials (ERPs), therefore allowing for a clear inspection of decision formation. Their approach revealed three neural signatures that appeared to follow three different stages of decision-making. First,

the occipital SSVEPs represented the encoding of sensory evidence by closely following the change in the stimulus. Second, a centro-parietal positivity (CPP) signal recorded from the midline electrodes showed a build-up that accelerated during the trial, reached a specific amplitude just prior to motor execution, and followed the sensory evidence even in the absence of a motor response. Due to these observations, the CPP was linked with the decision formation stage. Lastly, the limb movement selective beta-band activity was found to be representative of motor preparation. This study was the first human EEG work to identify a neural correlate of a supramodal decision-related signal that shows build-to-threshold dynamics similar to a decision variable and reflective of decision formation.

Following their seminal work, Kelly and O'Connell [27] observed that the properties (such as peak amplitude and buildup rate) of the CPP followed the strength of sensory evidence in a monotonic fashion in an RDM task, which provided further support for the role of CPP as a decision variable. In addition, they reported that the temporal build-up of the lateralized readiness potential (LRP) measured over the central electrode pairs (FC3/FC4 and C3/C4 pairs), which is considered a neural signature of unimanual motor preparatory activity [28], lagged the CPP even though these two ERPs shared similar build-to-threshold dynamics.

Since the establishment of the association between CPP and decision formation stage, other researchers have investigated the domain generality and task dependency of this signal using different experimental designs such as vibrotactile discrimination task [29], memory decisions (delayed-match-to-sample memory-based decision task) [30], contrast comparison task with an emphasis on speed pressure [31], prior-cued RDM task with evoked urgency component [32], contrast discrimination task with an awareness report (for rating clarification of perception) [33], and biological motion discrimination task [34]. In all of these studies, it was reported that the CPP signal followed the evidence accumulation stage. Therefore, these studies provided confirmation of the functional properties of CPP in decision-making.

The existence of studies supporting that CPP represents a decision variable raises the question of whether this neural signature has any relation with the

parameters defining the diffusion model. A recent study by van Vugt, Beulen, and Taatgen [30] reported a relation between the slopes in single-trial CPPs and the drift-rate parameter of DDM in their task requiring participants to make memory-based decisions. Considering this finding, it is worth considering the idea that the decision-making processes explained within the framework of the diffusion model can be tracked through CPP.

## 1.2 Perception and Understanding of Human Motion

The human brain is equipped with astonishing functioning mechanisms that enable the detection of a movement, discrimination of the animacy of the movement (whether it is performed by an organism or not), and understanding the intention behind that movement to decide and execute a proper response. Specifically, the movements of organisms (such as running, chasing, and gazing), particularly of animals and humans, show differing dynamics from other types of motion in the environment (such as mechanical motion). To underline this difference, the former movements have been classified under the term "Biological Motion" by the classical work of Johansson [35], where he introduced a method to study this class of actions using lightened points (later referred to as point-light displays (PLDs)) animations. Perception of biological movements, whether they include full-body movements such as running or chasing or include only a specific part of the body, such as facial expressions and hand gestures, hold a critical place in the survival of animals and humans.

### 1.2.1 Neural Basis of Biological Motion Perception

Any movement that characterizes an action of animals or humans can be categorized as an exemplar of biological motion. However, following the approach of Johansson [35], in experimental psychology, the phrase biological motion (BM)

has been typically used as an umbrella term for human movements animated using PLDs. Therefore, the abbreviation BM will be used under its correspondent implication in psychophysics throughout this section.

Two features define an action: form (that contains information defining the shape and structure of the object executing the movement; these objects can be a hand, a leg, or a whole body) and motion (that encompasses the notions as the position, speed, and heading direction of the object). To constitute a perception and understanding of an action, the defining features must be extracted from the visual stimuli and encoded properly. According to the classic two-pathway hypothesis, these features are processed in two parallel pathways stemming from the striate cortex and starting to differentiate in the extrastriate cortex [36] around the posterior inferior temporal sulcus (pITS) [37], which includes areas V3, V4, MT, and extrastriate body area (EBA). This hypothesis states that the form information is processed in the ventral pathway with the inferior temporal gyrus (IT) as the final hub, and the motion information is processed in the dorsal pathway that ends in the parietal cortex. As the features are successfully encoded in the posterior inferior temporal sulcus (pITS, which includes EBA and MT+), there is a strong suggestion that these two distinct feature representations converge at the superior temporal sulcus (STS) to be integrated to create representations of actions, an area when damaged or externally stimulated can result in impairments in the perception of BM [37]. Once the action representations are formed, the next step includes inferring the intention behind the movement since an action trajectory can be executed with many purposes, such as grasping a cup to drink a beverage, which differs from grasping a toy to play with it.

Understanding the goal of actions is considered to engage frontoparietal regions [37] where the frontal regions include the ventral premotor cortex (vPMC) and inferior frontal gyrus (IFG); the parietal regions consist of the inferior parietal lobule (IPL) and anterior intraparietal sulcus (aIPS). The vPMC has been observed to show selectivity in its response pattern that overlaps with the somatotopic organization of the body part representations [38, 39], which supports the view on vPMC being related to the encoding of the kinematics of the viewed actions. On the other hand, the organizations of the parietal regions [40, 41, 42] and the IFG

[41, 43] follow a more goal-tracking structure. In other words, the goal underlying the action is of more interest to these regions than the effector or the action itself. Therefore, IPL, aIPS, along with the IFG emerge as key areas for understanding observed human actions [37]. A body of studies has identified selectivity in the activity in distinct regions of the PPC as human participants passively observed naturalistic actions such as manipulation, locomotion, and skin-displacement actions [44]. Observing exemplars of manipulative hand actions have been found to activate the putative human anterior intraparietal (phAIP) area of the PPC [40, 45, 46], and this area was found to be invariant to the viewpoint [47]. Abdollahi et al. [45] showed that the observation of climbing action videos selectively activated the rosto-dorsal superior parietal lobule (SPL) site, whereas the same area was activated less when the observed actions belonged to the locomotion class. This study considered climbing as a distinct action class from locomotion; however, since the stimuli of these two classes shared similarities and the activations by the two action classes were largely coincident, climbing actions were suggested to be redefined under the locomotion class [44]. Therefore, the area SPL has been defined as being selective to the locomotion action exemplars. The last action class, the skin-displacement actions, includes the actions people execute toward their skin, such as scratching, massaging, or pitching. In their study, Ferri et al. [47] found a small region straddling the secondary somatosensory cortex (SII) and parietal area F, operculum (PFop) being selectively activated by observing skin-displacement actions.

### 1.2.2 Discrimination of Observed Natural Actions

Building on the functional organization of the observed action classes in the PPC, Platonov and Orban [48] designed a 2AFC task where the choice options were selected exemplars from a specific action class to probe whether the conclusions drawn from the passive observation tasks would have a correspondence in the behavioral responses of participants. In this study, the authors focused only on manipulative actions, and they created six versions of the main task by manipulating the stimuli either by injecting dynamic noise to create different versions

with various coherence levels (versions 1-5) or by changing the stimulus presentation duration (version 6). The first two experiments revealed that mean RT and percent accuracy rise with increasing coherence level; also, the RT and accuracy data of these versions could be explained closely by proportional rate diffusion models. Considering the definition of diffusion models, this close fit bore the implication of the existence of neurons selective to the observation of manipulation actions, and the authors reasoned that these neurons might exist within the action observation network for manipulation actions. The data from the third task, where the actions were displayed from either lateral or frontal views, complied with the invariance of the viewpoint in the phAIP [47]. The fourth and fifth tasks demonstrated that when actions were presented as videos, the discrimination thresholds were smaller compared to the cases where the static and motion information of the action was separately observed. The findings from the last version, where the action stimulus was interrupted at variable time instants, indicated that perception of action classes required a minimum exposure duration, which, if not met, decreased the accuracy performance. Overall, this study showed that the perception of observed actions differs from the perception of objects or scenes from several aspects, and the discrimination between observed actions can be explained closely with a diffusion model, which implies that formerly mentioned differences may be arising due to differences in the encoding of sensory evidence stage of the decision-making process.

To test the generability of results to other action classes, in their follow-up study [49], Platonov and Orban targeted two additional action classes: locomotion (exemplars: running and walking) and skin displacement (exemplars: massaging and scratching). To compare the discrimination processes involving these two action classes with the manipulation class (exemplars: rotating and rolling), the authors created the same coherence levels as in their previous design [48]. The mean RT and percent accuracy showed an increasing trend with the increasing amount of sensory strength. At the zero signal level, the RT value for the locomotion differed by almost twice as much from other action classes; however, that difference disappeared for the intact action stimuli.

A proportional rate diffusion model fit revealed several significant differences

between action classes in its model parameters. First, the model accounted for the striking differences in the RT, resulting in a significantly higher bound parameter for locomotion. The authors speculated that due to its ecological significance for a human to correctly detect a locomotion exemplar, the participants might have implicitly chosen to sacrifice speed to increase their performance for the locomotion class. Second, the accuracy threshold (defined as $0.55/kA'$ [9]) value for the skin-displacement actions was far higher than the two other classes. When ranked quantitatively, the threshold values resembled the ranking of the sizes of areas selective for the action classes of interest. Lastly, the drift rate significantly differed between manipulative hand actions and skin displacement, with manipulation having a much higher value that is in line with the differences in RT values between action classes.

Taken together, the results from the studies of Platonov and Orban provided concrete evidence for the applicability of diffusion models to explain data obtained from the discrimination of observed action exemplars for three action classes that have been found to selectively activate PPC. The close fit of diffusion models to the behavioral data boosted the idea that the differences between other higher-level vision and action observations are mainly due to the encoding of the sensory evidence stage, and the trends visible in the model parameters resonated with the findings and implications of previous neuroimaging studies.

## 1.3 Current Study

In this study, we investigated the neural correlates of the perception of naturalistic actions within the well-grounded theoretical framework of perceptual decision-making, utilizing EEG. We designed three experiments by adopting the paradigm used by Kelly and O'Connell [27], and in each of these experiments, the task was to discriminate between two exemplars of a specific action class. For the three experiments, we selected the action classes following the associations between the selectivity in the PPC and the diffusion model parameters in [49].

By incorporating the naturalistic-action perception into a perceptual decision-making paradigm, we had the following research questions (RQs) and hypotheses (Hs):

**RQ1. What are the decision-making stages that support the recognition of natural actions?**

**H1.** Building on the findings of studies that regarded action observation as a distinct aspect of higher-order vision and described this process as part of the sensory evidence accumulation phase of a decision-making process [44, 48, 49], we expected the decision-formation stage, where the encoded sensory evidence gets accumulated, of a decision-making process to be representative of the visual processing of the observed action exemplars. However, since the planning and the following execution of a motor response is merely a sensory process, we predicted that motor planning and execution stages would not actively support such a recognition process.

**RQ2. What are the neurophysiological bases of these processes?**

**H2.** Considering the literature on the neural correlates of perceptual decision making [26, 27, 32, 34], we expected that (1) the CPP signal, which is shown to be a neural signature of the decision formation in discrimination tasks, would track the recognition of observed actions, and (2) the LRP signal, which is an ERP correlate of motor preparation related activity, to represent the activity related to the response execution and merely depend on the sensory evidence accumulation stage.

**RQ3. Are these processes similar to or different from those demonstrated using simpler motion stimuli in the domain of perceptual decision-making?**

**H3.** Given the sensitivity of the evidence accumulation phase of decision-making to stimulus strength, we expected that as the CPP signal grows, as a representative of the integration of evidence, it would track the level of signal strength (i.e., coherence) and thus show a consistent build-up pattern with the

findings of previous literature. However, considering a recent study by Oguz, Aydin, and Urgen [34] on BM direction discrimination, which reported a later onset on the CPP build-up (approximately at 350 ms) compared to simpler discrimination tasks (approximately between 200 - 300 ms) [26, 27], we expected to see a later onset than that was observed in the BM direction discrimination task given the ecological validity of natural actions. In addition to the integration-to-bound property of the CPP, its amplitude should converge to a specific threshold value at the time of response execution due to its definition as a DV. Therefore, regardless of the level of sensory strength, we predicted the CPP to reach specific bounds in each experiment. Similarly, we expected the LRP signal to carry the same signal strength-independent behavior when probed prior to response execution.

**RQ4. How do decision-making processes and their neural bases differ in the recognition of different action classes?**

**H4.** Considering the findings that established different regions in the PPC to be representative of distinct action observations and the sizes of these regions, we expected that such differences would impact the decision-formation stage and thus would reflect on the properties (mean amplitude, peak amplitude, and onset latency) of the CPP signal.

# Chapter 2

# Methods

## 2.1 Participants

Twenty participants (11 female, age 25.5±4.29) were recruited for the current study. The eligibility criteria were the following: (i) having normal or corrected to normal vision, (ii) having no history of neurological or psychiatric medications, and (iii) having no medical implants on body parts above the neck. Eligible participants received a briefing about the procedures that will be followed in both behavioral and EEG sessions prior to experiment scheduling. Upon agreement, they provided written informed consent forms (one per each type of session) and a pre-screening form before the beginning of the study. The study was approved by the Human Research Ethics Committee of Bilkent University. Each participant attended four sessions in different days. The order of the action sessions was counterbalanced in behavioral and EEG experiments separately. Due to the excessive amount of artifacts in the EEG data, three participants were excluded from the study. Thus, the analyses focused on the data of seventeen participants.

## 2.2 Stimuli

The experimental stimuli consisted of videos displaying human actors performing natural actions from a lateral view. The actors were trained to perform the actions in the same movement trajectory (beginning from the starting position of an action to the ending position) with similar speeds. Each action began and ended in the same position, lasting for two seconds. The stimuli videos were recorded in front of a wall-sized gray curtain (to minimize distractions) in a room without windows to prevent lighting-related issues.

The action exemplars were selected from three action classes of interest: massaging and scratching (skin-displacement), walking and running on the spot (locomotion), and pushing and dragging (manipulative hand). Four versions (2 actors x 2 variants) per action exemplar were generated to increase variation in the stimuli. The two variants in each action class were the following: the targeted body area (either head or chest) in skin-displacement actions; the direction of the movement (either left or right) in the locomotion actions; and the object that the manipulation action was realized on (either a cup or a cubic). The locomotion videos captured the full bodies of the actors (female and male), whereas, for the manipulation and skin-displacement actions, only the upper bodies of the actors were recorded. The recorded videos were then imported into MATLAB2021b [50] workspace to adjust their dimensions, sizes, and central points so that the positioning of the actors matched and the actions took place at the center of each frame. To correct a sudden lighting issue in an exemplar of the locomotion class, the functions of the SHINE toolbox [51] were utilized in all locomotion stimuli.

In order to manipulate the coherence (signal-to-noise ratio), following the previous work [48], each pixel of each frame of each video, the current pixel, was assigned with a random probability of swap, and this random value was then compared to a threshold to decide whether that specific pixel would be swapped with another pixel (a candidate pixel) or not. The candidate pixel was randomly selected from the pixels within a circle whose center was the current pixel, with its radius determined by a distance parameter (set to 316 pixels). Using

this method, various versions of each action video with different coherence levels (CL) were generated.

Utilizing this algorithm, two types of stimuli were generated for this study: the target motion (TM) stimuli and the scrambled motion (SM) stimuli. The TM stimuli consisted of videos displaying actions (i.e., all sixty frames of an exemplar were included) with five different CLs (50, 35, 20, 15, and 9) for each exemplar, and the coherence manipulation was done by applying the algorithm on successive frames of each exemplar video. The SM stimuli consisted of videos comprising the same frame (only the starting frame) of an action with four different CLs (0, 4, 7, and 10), and the coherence manipulation was done by applying the algorithm on a specific frame for thirty iterations. The aim of the SM stimuli was to eliminate any sensory-evoked potentials that would occur otherwise at the beginning of the target stimuli presentation. To achieve this, a smooth transition from the SM presentation to the TM presentation was established by generating a separate timing sequence of SM stimuli per each coherence level of TM stimuli.

In the end, forty TM stimulus videos (5 coherence levels x 2 actors x 2 exemplars x 2 variants) and thirty-two SM stimulus videos (4 coherence levels x 2 actors x 2 exemplars x 2 variants) were generated. As the final step, the edges of all frames of TM and SM videos were gradually blurred into the background color of the experiment (RGB color code: [150 150 150]). Figures 2.1, 2.2, 2.3 display snapshots of the five coherence levels for two exemplars from TM stimuli sets for the skin displacement, locomotion, and manipulation actions, respectively.

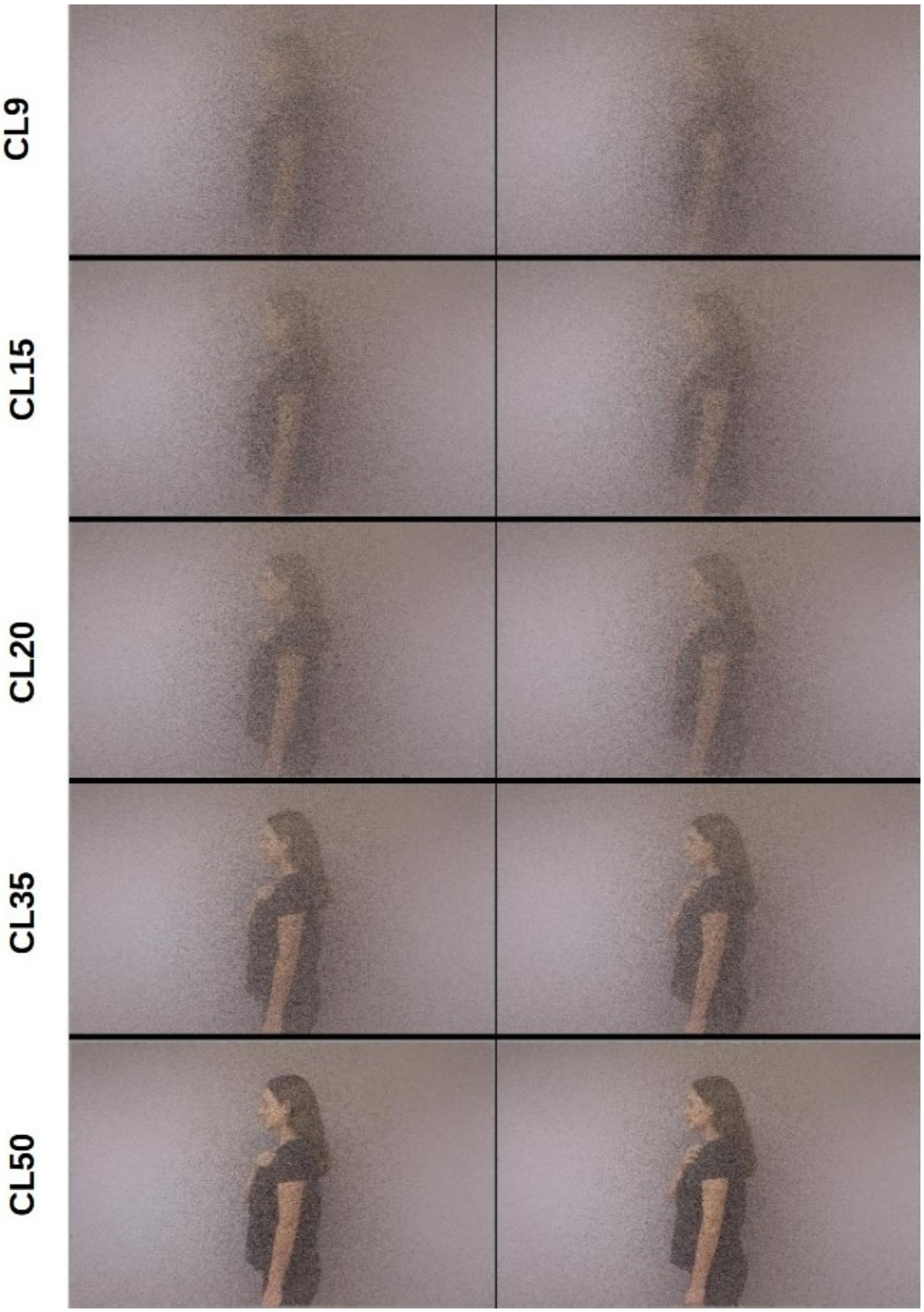


Figure 2.1: Snapshots from the Exemplars of Skin-Displacement Action Class

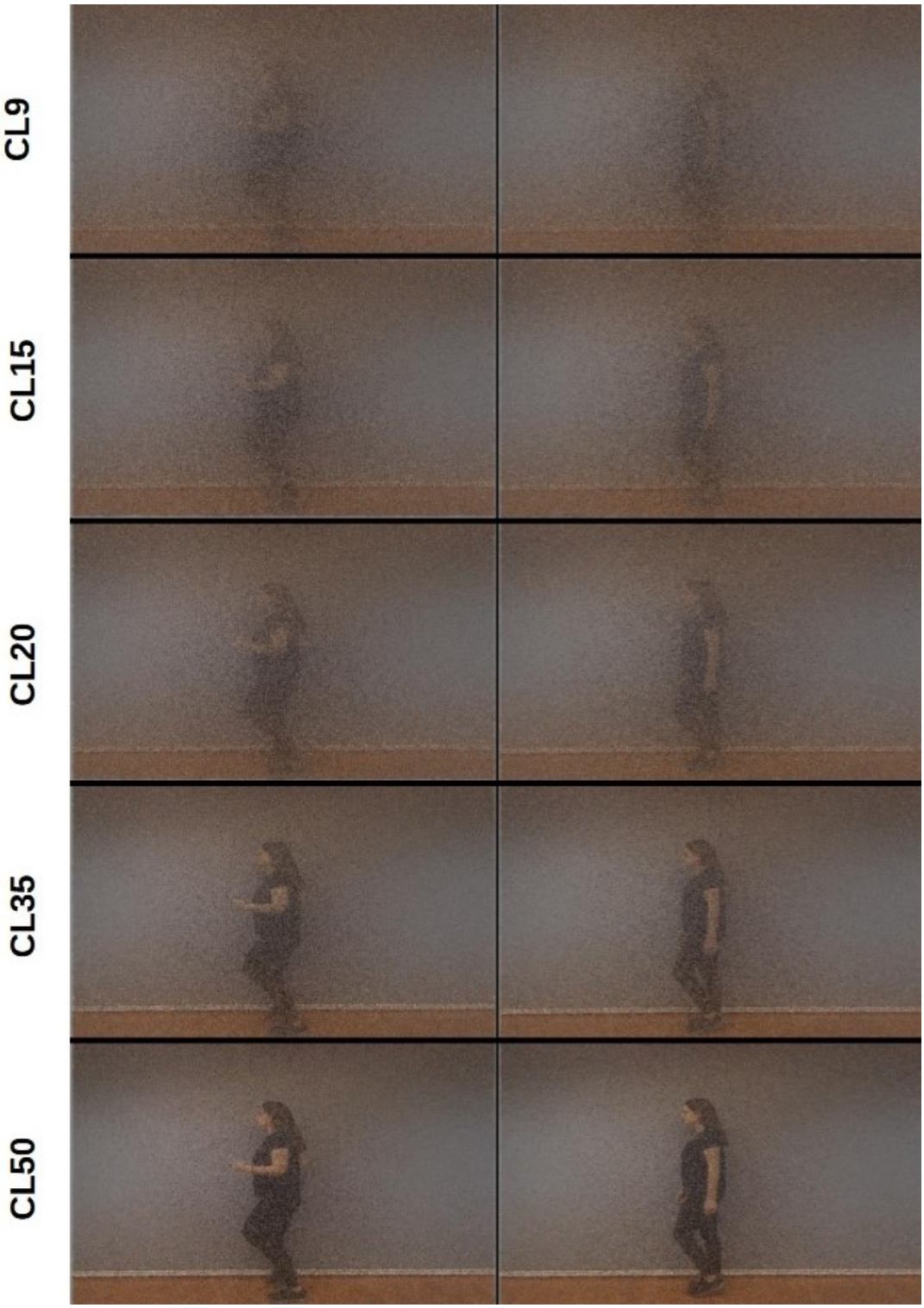


Figure 2.2: Snapshots from the Exemplars of Locomotion Action Class

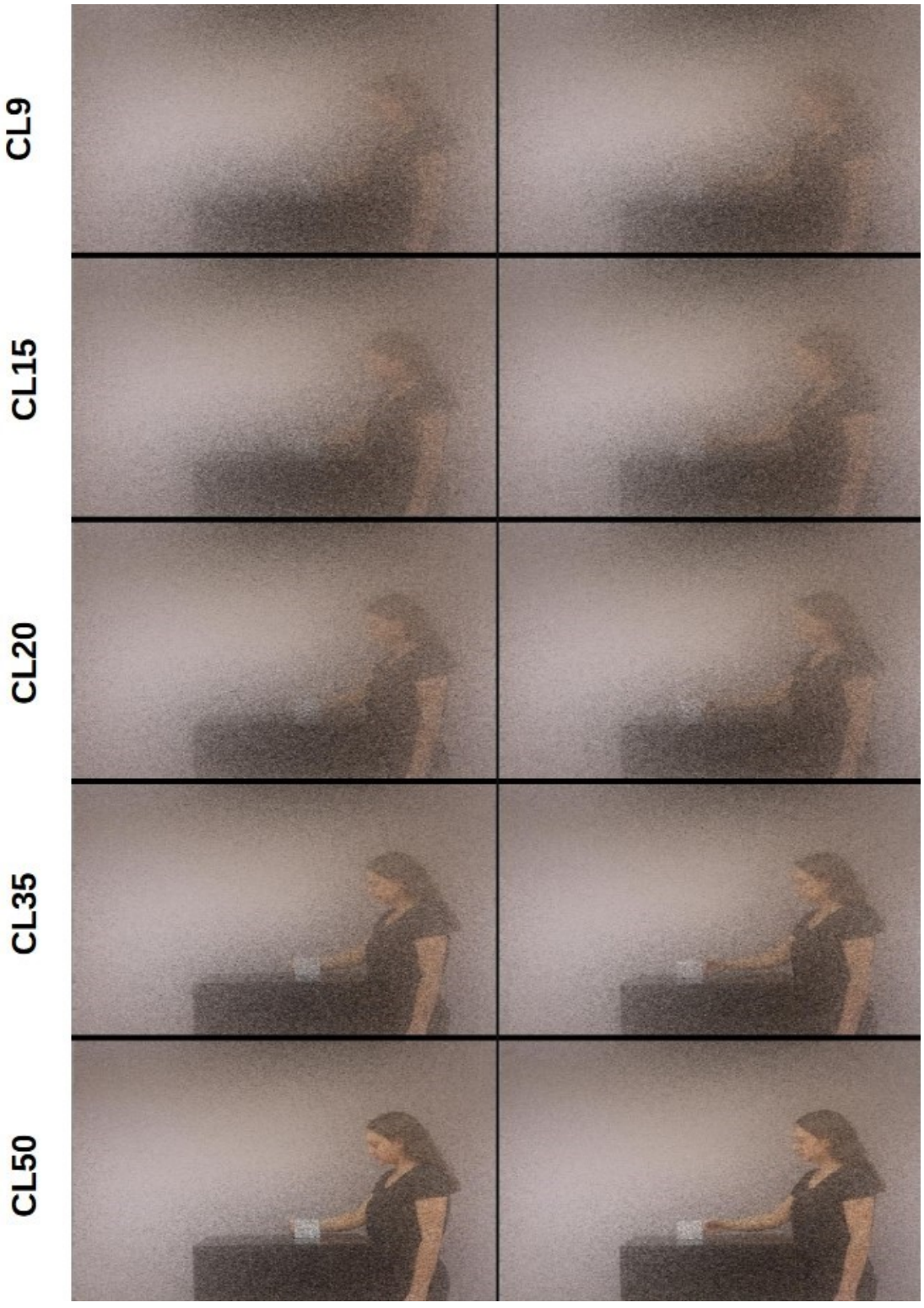


Figure 2.3: Snapshots from the Exemplars of Manipulative Hand Action Class

## 2.3 Experimental Paradigm and Procedure

The experiment paradigm was built on the structure of widely used two-alternative forced choice tasks. In our study, the choice options were action exemplars of a particular action class. For the manipulative hand action class experiment, the exemplars were *dragging* and *pushing* actions; for the locomotion action class experiment, they were *running* and *walking* and for the skin-displacement action class the exemplars were *massaging* and *scratching*.

In line with the previous work [27], a trial began with a fixation dot located at the center of the screen for 1 second; it was then followed by an SM stimulus for a variable length of duration between 3-6 seconds where the duration varied in each trial to prevent the participants from anticipating the timing of the appearance of the TM stimulus. After the SM stimulus, a TM stimulus was shown on the display for a maximum duration of 2.5 seconds, and participants were required to respond during this period. The flow of a trial for discrimination of manipulation exemplars is depicted in Figure 2.4.

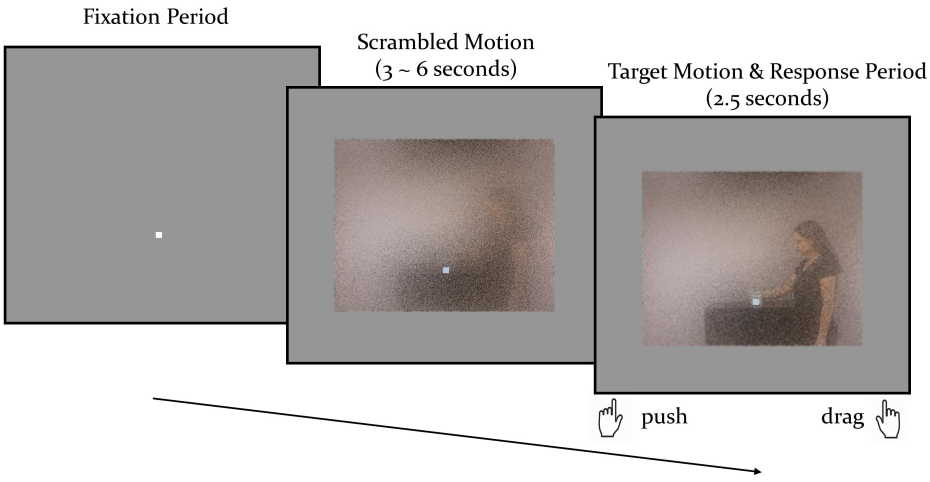


Figure 2.4: An Example Trial Flow from Manipulation Class

The task was to discriminate between action exemplars from an action class and press the related button (either key 'D' or key 'L') on the keyboard as soon as the participants were ready to report their decision. If the participants failed to respond within 2.5 seconds to a trial, then that trial was classified as a missed

trial, and the subsequent trial began.

The study consisted of four sessions: a behavioral session where the participants participated in three consecutive experiments and three EEG sessions booked for separate days. Each experiment included two training blocks with feedback and several experimental blocks without feedback. The number of experimental blocks differed in behavioral and EEG sessions; each experiment included two experimental blocks in the behavioral session, whereas there were six blocks in the EEG sessions.

In each experiment, the order of TM stimuli was pseudo-randomized by applying the following two rules: 1. two consecutive actions cannot be of the same exemplar with the same coherence level, 2. the possibility of any exemplar-coherence combination pair cannot exceed the number of trials per combination that was previously defined. In behavioral sessions, this number was defined as 2 (64 trials divided by 32 pairs), whereas it was 12 in EEG sessions (384 trials divided by 32 combinations). The order of the SM stimuli was fully randomized.

**A behavioral session** was included before EEG sessions to check whether the participants could pass a 75% accuracy threshold in each coherence level of each action class (except the skin-displacement actions class)—failure to pass the threshold led to being excluded from continuing the following sessions. The behavioral session took place in a dark room equipped with an MSI laptop PC (model: CX62 6QD) and an external monitor (Philips model: M822xVQ1T, 60Hz). The instructions related to the upcoming part of the behavioral session were provided to the participants prior to the beginning. Participants were free to give breaks within the current part in between the blocks and between consecutive parts of the session. The order of participation in the three parts was counterbalanced across participants, and the order was repeated every six participants. The behavioral session consisted of three sections, which were designed as shortened versions of the EEG experiments. Each section comprised two subsequent training parts; the first training part was admitted to ease the understanding of the nature of the task and learning of the response keys; thus, the relevant TM stimuli were displayed with the highest coherence levels used in this study (i.e.,

CL50), in the second part the experimental TM stimuli levels (CL9, CL15, CL20, and CL35) were introduced. Each relevant TM stimulus was shown only once in the training parts; therefore, there were forty trials (eight in the first part and thirty-two in the second part). After each trial, participants received feedback on their responses as correct, incorrect, or missed. The training parts were followed by two experimental parts - each with thirty-two trials- where only the experimental TM stimuli levels were displayed, and no feedback was provided after responses. The accuracy scores of the participants were computed by dividing the correct trials by the total number of trials (sixty-four) of the experimental blocks. Each section lasted approximately ten minutes, and a behavioral session was completed in approximately forty minutes (including the breaks). A behavioral session was classified as successful if the threshold criteria were met for all four levels of two action classes.

**EEG sessions** took place subsequent to a successful behavioral session, and each EEG session was booked for a separate day. The EEG sessions took place in a dark room equipped with an IPS monitor (The Dell Alienware AW2720HF, 27 inches, 60 Hz) located 57 cm away from a chin-rest positioned to keep the head of the participant stable. The order of participation in the EEG sessions was counter-balanced across participants, and similar to behavioral session parts, the order was repeated for every six participants. Participants completed the same tasks in EEG experiments as they did in the behavioral session. All EEG experiments included two training parts, structured exactly the same as the behavioral session, and six experimental parts where the number of trials per block and the number of blocks were increased to sixty-four and six, respectively. Therefore, disregarding the training parts, there were 384 trials in an EEG session where each of the four coherence levels was shown 96 times.

## 2.4 EEG Data Acquisition and Preprocessing

Continuous EEG data was recorded from 64 scalp electrodes with a sampling rate of 1000 Hz. The FCz electrode was selected as the reference and FPz as the

ground during the recordings. All impedance values were kept below 18kΩ.

Offline processing of the raw data was performed by utilizing the functions of the EEGLAB toolbox [52] and the ERPLAB toolbox [53]. A classic FIR (finite impulse response) low-pass filter with a 3dB cut-off frequency of 40 Hz was applied to the data to remove non-electrophysiological high-frequency components (e.g., channel noise). Then, data was visually inspected for detection and manual removal of artifacts (muscle movements, unusual patterns, etc.) and bad channels. The data was high-pass filtered with a 3dB cut-off frequency of 0.5Hz (classic FIR filter) to eliminate artifacts with slow drifts. Subsequently, independent component analysis was applied to continuous data using the Runnica algorithm to remove further artifacts. The missing channels were interpolated using the spline interpolation method; then, the data was re-referenced to the average reference.

For the CPP analysis, two datasets were obtained by separately binning the pre-processed data into four different event sequences according to the CL of the stimulus (CL35, CL20, CL15, and CL9); the first dataset was binned to include the intervals that began with the onset of a TM stimulus and ended with a correct response, the second dataset was binned to include the intervals began with the onset of a correct answer that was preceded by a TM stimulus. These two datasets were then epoched to two different time intervals: (i) from -100 ms to 999 ms relative to stimulus onset and (ii) from -999 ms to 100 ms relative to response onset.

For the LRP analysis, similar to the CPP waveforms, two datasets were obtained by binning the pre-processed data into eight different event sequences depending on the CL of the target stimulus and the hand the response was reported (left or right). The stimulus-locked dataset was epoched from -100 ms to 999 ms relative to the onset of the stimulus, and the response-locked dataset was epoched from -999 ms to 100 ms relative to the response onset. Baseline corrections were applied to the range of -100 ms to 0 ms relative to stimulus presentation in the datasets locked to stimulus onset; no correction was performed for the others.

## 2.5 Data Analysis

### 2.5.1 Behavioral Data Analysis

The behavioral dependent variables of this study were the mean response time and percentage of miss-rate, and these behavioral metrics were analyzed for each coherence level and action class. The behavioral data from three experiments were merged into a single dataset prior to outlier inspection. Before the analyses, missed trials (where the participant failed to respond) and trials with response time higher than 2.1 seconds and lower than .1 seconds were excluded from the data.

Response time was defined as the duration that began with the appearance of the first frame of a TM stimulus and ended either with a motor response or with the removal of the last frame of the TM stimulus from the display. Only the trials with correct answers were included in the response time analysis. The miss rate was defined as the proportion of the trials where participants failed to respond during the response window, and this measure was considered as an indicator of the perceived difficulty of the stimulus. The percentage of miss-rate for each coherence level was computed by dividing the number of missed trials by the number of trials in that coherence level.

To investigate how the action class variability and different coherence levels impacted the mean response time, a two-way 3x4 Repeated Measures Analysis of Variance (R-ANOVA) was applied. On the other hand, a Shapiro-Wilk test applied to the percentage miss-rate data revealed a significant deviation from normal distribution ($W = .81$, $p < .001$). Therefore, the impact of each independent variable on the miss-rate was assessed by applying Friedman's test, which is the non-parametric equivalent of one-way repeated measures ANOVA.

### 2.5.2 ERP Analysis

Since the aim of the study was to track the neural markers active in the decision process, the two neural signals that show decision-related build-to-threshold dynamics were of interest: the CPP as a representative of the decision variable and the LRP as an indicator of the motor preparation. These neural markers were investigated in two different time intervals by time-locking the waves to either the onset of stimulus or the onset of motor response. After time-locking, the CPP and LRP waveforms were computed by taking the grand average of the individual ERPs obtained by averaging each participant's epoched data sets.

#### CPP Analysis

Following the convention in the literature [27], the CPP analysis focused on the CPz and its bilateral electrodes (CP1 and CP2). A visual inspection of the stimulus-locked grand-averaged ERP waveforms covering the time interval of -100 ms to 1000 ms revealed a build-up between 200 - 300 milliseconds in each experiment data. However, the response-locked grand-averaged ERPs covering the -1000 ms to 100 ms interval revealed differences in the time course of CPP build-up between experiments. To discover the time course where the significant differences between coherence levels start to appear on ERPs (both the stimulus-locked and the response-locked) read from the centroparietal electrodes, the three individual ERP sets of each participant were subjected to a factorial mass-univariate analysis utilizing false-discovery rate (FDR) correction with factors of coherence level and action class. Then, the mean amplitude of CPP was computed by taking the average of the centroparietal channels over 300-800 ms following the stimulus onset and over -300 milliseconds to the onset of response execution to obtain a metric to be used for assessing integration-to-threshold dynamics. A two-way R-ANOVA was separately conducted on the mean CPP amplitude obtained from these two waveforms with factors of action class (three levels) and coherence levels (four levels).

### LRP Analysis

The LRP was assessed over two pairs of electrodes: the FC4-FC3 and the C4-C3. A difference wave was obtained by subtracting the ipsilateral signal from the contralateral signal to compute the LRP. The contra and ipsi regions were defined with respect to the hand that initiated the response. Like the CPP analysis, we performed factorial mass-univariate analysis utilizing FDR correction with factors of coherence level and action class on the individual ERP sets.

# Chapter 3

# Results

In this chapter, behavioral findings from mean response time and percent miss rate will be presented first. Following, the analyses related to Centro Parietal Positivity and Lateralized Readiness Potential will be presented.

## 3.1 Behavioral Results

### 3.1.1 Response Time

To investigate the effect of the action class and coherence level of the stimulus on the response time of the participants, we run a 3 (action class) x 4 (coherence level) R-ANOVA. The results showed the main effects of the coherence level ($F(1.701,27.218) = 244.430$, $p < .001$, $\eta^2 = .736$) and action class ($F(1.861,29.783) = 4.071$, $p = .03$, $\eta^2 = .024$). In addition, the analysis revealed a significant interaction between the action class and coherence ($F(2.816,45.054)=36.091$, $p < .001$, $\eta^2 = .068$), which is also visible in the plot given in Figure 3.1 demonstrating the mean RT values within and between both coherence levels and action-classes.

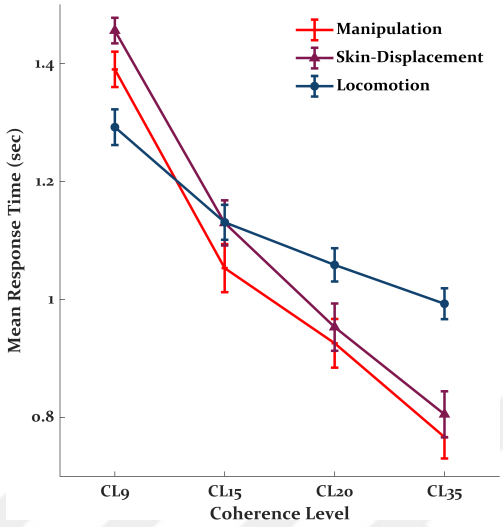


Figure 3.1: The Change in the Mean Response Time Across Coherence Levels and Action Classes

Bonferroni corrected post-hoc comparisons on the levels of action class variable revealed that the average time required to discriminate between two exemplars of manipulation class ($M$=1.034, $SD$=.140) was slightly smaller than the time elapsed during the discrimination of exemplars of locomotion class ($M$=1.119, $SD$=.115). In contrast, the remaining comparisons did not significantly differ (see Table 3.1).

Table 3.1: Post-Hoc Comparisons Between the Levels of Action Class on the Mean Response Time

| | | Mean Difference | SE | t | $p_{bonf}$ | |
|---|---|---|---|---|---|---|
| Man | Skin | -.052 | .030 | -1.742 | .273 | |
| | Loc | -.085 | .030 | -2.828 | .024 | * |
| Skin | Loc | -.033 | .030 | -1.087 | .856 | |

*Note.* P-value adjusted for comparing a family of 3

*Note.* Results are averaged over the levels of *Coherence*

*Note.* The abbreviations *Man*, *Skin*, *Loc* refer to manipulation actions, skin-displacement actions, and locomotion actions, respectively.

Post-hoc comparisons on the coherence levels revealed significant differences between all pairs, with a trend of the conditions with smaller coherence levels having significantly higher average response times than those with larger coherence

levels as presented in Table 3.2.

Table 3.2: Post-Hoc Comparisons Between the Levels of Coherence on the Mean Response Time

| | | Mean Difference | SE | t | $p_{bonf}$ | |
|---|---|---|---|---|---|---|
| CL9 | CL15 | .275 | .020 | 13.539 | <.001 | *** |
| | CL20 | .400 | .020 | 19.719 | <.001 | *** |
| | CL35 | .524 | .020 | 25.837 | <.001 | *** |
| CL15 | CL20 | .125 | .020 | 6.180 | <.001 | *** |
| | CL35 | .250 | .020 | 12.298 | <.001 | *** |
| CL20 | CL35 | .124 | .020 | 6.119 | <.001 | *** |

*Note.* P-value adjusted for comparing a family of 6

*Note.* Results are averaged over the levels of *Action Class*

Furthermore, the post hoc comparisons of the interaction effect on the mean response time revealed differences within action classes due to coherence levels, as depicted in Figure 3.1 and presented in Table 3.3, The mean response time decreased significantly as the coherence level of the stimulus increased in the manipulation action class; the same performance pattern was also observed in the skin-displacement action class. For the locomotion action class discrimination, participants took significantly longer to discriminate in the lowest coherence level compared to consecutive higher levels; the differences observed in the mean response between other coherence levels did not reach significance ($\alpha = .05$). Overall, the interaction effects indicated an increased task difficulty within each action class with decreasing coherence level.

Table 3.3: Post-Hoc Comparisons for the Interaction of Action Class x Coherence on the Mean Response Time

| | | Mean Difference | SE | t | $p_{bonf}$ | |
|---|---|---|---|---|---|---|
| Man CL9 | Skin CL9 | -.066 | .034 | -1.909 | 1 | |
| | Loc CL9 | .098 | .034 | 2.844 | .413 | |
| | Man CL15 | .337 | .026 | 13.011 | <.001 | *** |
| | Skin CL15 | .26 | .038 | 6.789 | <.001 | *** |

| | | | | | | |
|---|---|---|---|---|---|---|
| | Loc CL15 | .259 | .038 | 6.765 | <.001 | *** |
| | Man CL20 | .464 | .026 | 17.929 | <.001 | *** |
| | Skin CL20 | .437 | .038 | 11.399 | <.001 | *** |
| | Loc CL20 | .332 | .038 | 8.647 | <.001 | *** |
| | Man CL35 | .623 | .026 | 24.067 | <.001 | *** |
| | Skin CL35 | .585 | .038 | 15.252 | <.001 | *** |
| | Loc CL35 | .397 | .038 | 1.364 | <.001 | *** |
| Skin CL9 | Loc CL9 | .164 | .034 | 4.753 | <.001 | *** |
| | Man CL15 | .403 | .038 | 1.506 | <.001 | *** |
| | Skin CL15 | .326 | .026 | 12.587 | <.001 | *** |
| | Loc CL15 | .325 | .038 | 8.48 | <.001 | *** |
| | Man CL20 | .53 | .038 | 13.829 | <.001 | *** |
| | Skin CL20 | .503 | .026 | 19.411 | <.001 | *** |
| | Loc CL20 | .397 | .038 | 1.362 | <.001 | *** |
| | Man CL35 | .689 | .038 | 17.976 | <.001 | *** |
| | Skin CL35 | .651 | .026 | 25.114 | <.001 | *** |
| | Loc CL35 | .463 | .038 | 12.079 | <.001 | *** |
| Loc CL9 | Man CL15 | .239 | .038 | 6.234 | <.001 | *** |
| | Skin CL15 | .162 | .038 | 4.232 | .004 | ** |
| | Loc CL15 | .161 | .026 | 6.228 | <.001 | *** |
| | Man CL20 | .366 | .038 | 9.557 | <.001 | *** |
| | Skin CL20 | .339 | .038 | 8.842 | <.001 | *** |
| | Loc CL20 | .233 | .026 | 9.014 | <.001 | *** |
| | Man CL35 | .525 | .038 | 13.704 | <.001 | *** |
| | Skin CL35 | .487 | .038 | 12.696 | <.001 | *** |
| | Loc CL35 | .299 | .026 | 11.555 | <.001 | *** |
| Man CL15 | Skin CL15 | -.077 | .034 | -2.227 | 1 | |
| | Loc CL15 | -.078 | .034 | -2.254 | 1 | |
| | Man CL20 | .127 | .026 | 4.918 | <.001 | *** |
| | Skin CL20 | .1 | .038 | 2.608 | .725 | |
| | Loc CL20 | -.006 | .038 | -.144 | 1 | |
| | Man CL35 | .286 | .026 | 11.056 | <.001 | *** |
| | Skin CL35 | .248 | .038 | 6.462 | <.001 | *** |

| | | | | | | |
|---|---|---|---|---|---|---|
| | Loc CL35 | .06 | .038 | 1.573 | 1 | |
| Skin CL15 | Loc CL15 | -97.53 | .034 | -.027 | 1 | |
| | Man CL20 | .204 | .038 | 5.324 | <.001 | *** |
| | Skin CL20 | .177 | .026 | 6.823 | <.001 | *** |
| | Loc CL20 | .071 | .038 | 1.858 | 1 | |
| | Man CL35 | .363 | .038 | 9.471 | <.001 | *** |
| | Skin CL35 | .324 | .026 | 12.527 | <.001 | *** |
| | Loc CL35 | .137 | .038 | 3.575 | .041 | * |
| Loc CL15 | Man CL20 | .205 | .038 | 5.349 | <.001 | *** |
| | Skin CL20 | .178 | .038 | 4.635 | <.001 | *** |
| | Loc CL20 | .072 | .026 | 2.786 | .417 | |
| | Man CL35 | .364 | .038 | 9.496 | <.001 | *** |
| | Skin CL35 | .325 | .038 | 8.488 | <.001 | *** |
| | Loc CL35 | .138 | .026 | 5.327 | <.001 | *** |
| Man CL20 | Skin CL20 | -.027 | .034 | -.795 | 1 | |
| | Loc CL20 | -.133 | .034 | -3.857 | .020 | * |
| | Man CL35 | .159 | .026 | 6.138 | <.001 | *** |
| | Skin CL35 | .12 | .038 | 3.139 | .16 | |
| | Loc CL35 | -.067 | .038 | -1.75 | 1 | |
| Skin CL20 | Loc CL20 | -.106 | .034 | -3.062 | .225 | |
| | Man CL35 | .186 | .038 | 4.861 | <.001 | *** |
| | Skin CL35 | .148 | .026 | 5.703 | <.001 | *** |
| | Loc CL35 | -.04 | .038 | -1.035 | 1 | |
| Loc CL20 | Man CL35 | .292 | .038 | 7.614 | <.001 | *** |
| | Skin CL35 | .253 | .038 | 6.606 | <.001 | *** |
| | Loc CL35 | .066 | .026 | 2.541 | .824 | |
| Man CL35 | Skin CL35 | -.039 | .034 | -1.122 | 1 | |
| | Loc CL35 | -.226 | .034 | -6.561 | <.001 | *** |
| Skin CL35 | Loc CL35 | -.187 | .034 | -5.439 | <.001 | *** |

*Note.* P-value adjusted for comparing a family of 66

*Note.* The abbreviations *Man*, *Skin*, *Loc* refer to manipulation actions, skin-displacement actions, and locomotion actions, respectively.

### 3.1.2 Miss Rate

The percentage miss-rate showed a declining pattern with increasing coherence level in each action class, as depicted in Figure 3.2. A Friedman's test on the miss-rate data with action class as a factor revealed significant differences among the three action classes ($\chi^2(2) = 27.791$, $p < .001$, $W = .817$). The pairwise comparisons using the Wilcoxon Signed Rank test revealed that the median miss rate score of the skin displacement action class ($MD = 10.40$) was significantly different from the median miss rate scores of the manipulation actions ($MD = .89$) and locomotion class ($MD = .27$) with $p < .001$. Meanwhile, the difference in the median scores for manipulation and locomotion failed to reach the significance threshold ($\alpha = .05$).

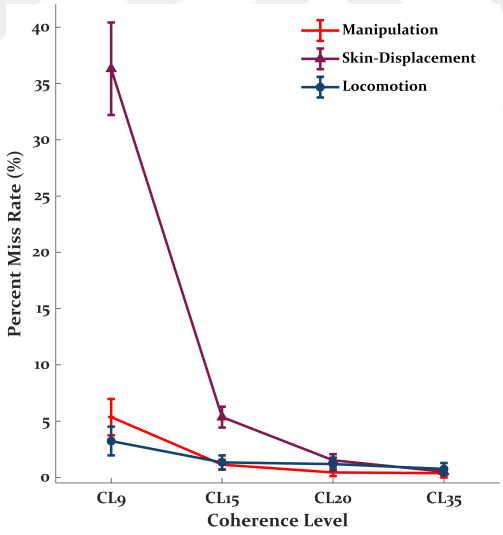


Figure 3.2: The Change in the Percent Miss-Rate Across Coherence Levels and Action Classes

A separate Friedman's test on the miss-rate scores with coherence as a factor revealed significant differences between coherence levels ($\chi^2(3) = 44.159$, $p < .001$, $W = .866$). Following pairwise comparisons using the Wilcoxon Signed Rank test revealed that the median score of CL9 ($MD = 11.35$) significantly differed from the median scores of CL15 ($MD = 1.85$), CL20 ($MD = .35$) and CL35 ($MD = 0.00$) with $p < .001$ in each comparison. Similarly, the median score of CL15 differed significantly from the median scores of CL20 ($p < .01$) and CL35 ($p < .01$).

## 3.2 ERP Results

In this section, the results of the analysis of ERP components will be presented in the order of CPP, followed by LRP. First, for both stimulus-locked and response-locked analyses of the CPP signal, the time course of the evolving CPP signal will be presented. Then, the results of factorial mass univariate analyses used to determine the time interval for the mean amplitude computation will be presented. Finally, the results of the analyses on the mean amplitude metric will be given. For the second ERP, the LRP, as no significant results were obtained, only the time course of stimulus-locked and response-locked LRPs will be presented for each action class.

### 3.2.1 Centro Parietal Positivity

#### 3.2.1.1 Stimulus-Locked Analysis

The CPP was observed to show a build-up starting around 200-300 milliseconds after the stimulus onset in all action-class experiments, with its peak following the coherence level of the stimulus (Figure 3.3).

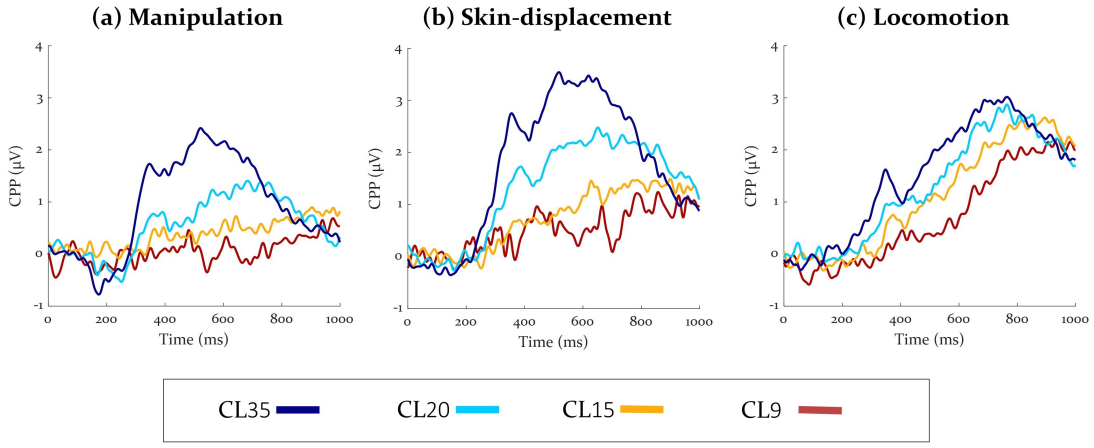


Figure 3.3: Stimulus-Locked Grand-Averaged CPPs Across Action Classes

A 3x4 factorial mass univariate analysis - with factors action class and coherence - of the stimulus-locked ERPs over the centroparietal electrodes supported the visual inspection of the ERPs by revealing significant main effects of action class (Figure 3.4) and of coherence levels (Figure 3.5) over the time range 300-800 ms.

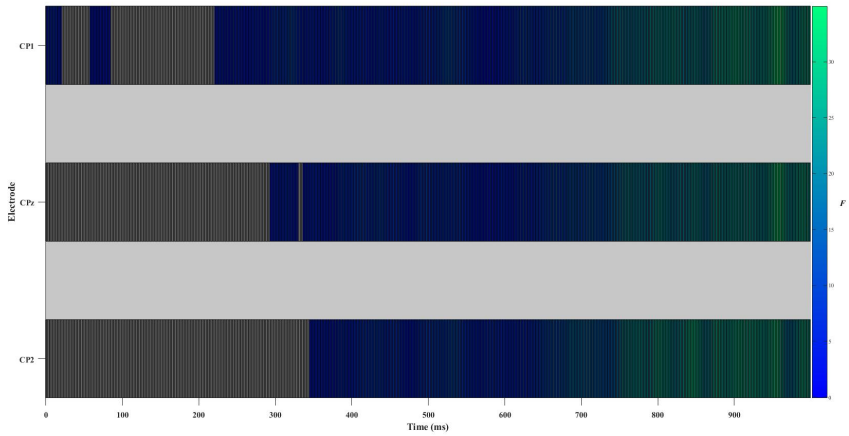


Figure 3.4: Factorial Mass Univariate Analysis of Stimulus-Locked CPP Over Centro Parietal Channels, *Displaying the Main Effect of Action Class*

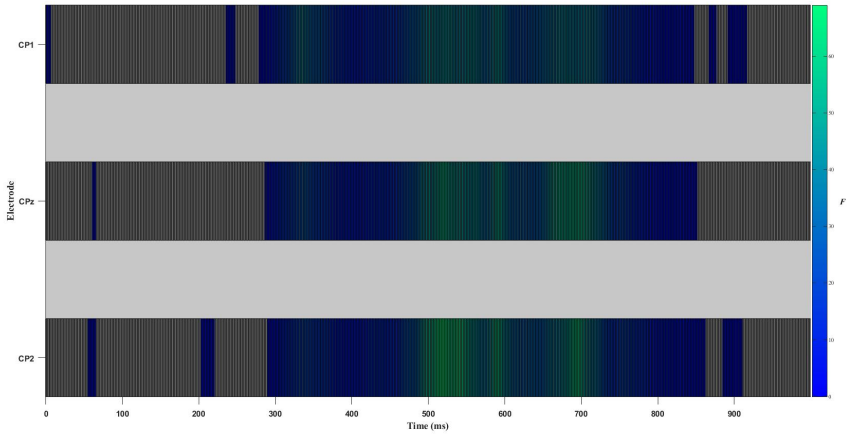


Figure 3.5: Factorial Mass Univariate Analysis of Stimulus-Locked CPP Over Centro Parietal Channels, *Displaying the Main Effect of Coherence*

A 3 (action class) x 4 (coherence level) R-ANOVA on the mean amplitude of the stimulus-locked CPP on the time range 300-800 milliseconds revealed the

main effects of action class ($F(1.880, 30.085) = 12.520$, $p < .001$, $\eta^2 = .118$) and coherence level ($F(2.084, 33.352) = 59.563$, $p < .001$, $\eta^2 = .445$) with a significant interaction of action class and coherence level ($F(2.848, 45.574) = 4.121$, $p < .05$, $\eta^2 = .034$). Post-hoc comparisons on the level of action class indicated that the mean CPP amplitude was significantly lower for manipulation ($M = .783$, $SD = .689$) actions compared to exemplars belonging to skin-displacement ($M = 1.569$, $SD = .760$) and locomotion ($M = 1.440$, $SD = .822$) classes. Post-hoc comparisons on the coherence levels resulted in significant differences between all pairs, with a trend of the conditions with smaller coherence levels having significantly lower mean CPP amplitudes than those with larger coherence levels as presented in Table 3.4.

Table 3.4: Post-Hoc Comparisons Between the Levels of Coherence on the Mean Stimulus-Locked CPP Amplitude

| | | Mean Difference | SE | t | $p_{bonf}$ | |
|---|---|---|---|---|---|---|
| CL9 | CL15 | -.433 | .142 | -3.056 | <.05 | * |
| | CL20 | -1.060 | .142 | -7.483 | <.001 | *** |
| | CL35 | -1.776 | .142 | -12.534 | <.001 | *** |
| CL15 | CL20 | -.627 | .142 | -4.427 | <.001 | *** |
| | CL35 | -1.343 | .142 | -9.478 | <.001 | *** |
| CL20 | CL35 | -.716 | .142 | -5.051 | <.001 | *** |

*Note.* P-value adjusted for comparing a family of 6

*Note.* Results are averaged over the levels of *Action Class*

The post hoc comparisons of the interaction effect on the mean stimulus-locked CPP amplitude (given in Table 3.5) revealed that the mean stimulus-locked CPP amplitude in the manipulation action class mainly differed significantly between coherence levels with a pattern of condition with higher coherence level having higher mean amplitude. A similar pattern with stronger significance was observed for the relation between mean CPP amplitude and coherence levels in the skin-displacement action class. However, the mean CPP amplitude in the locomotion class differed significantly for the pairs that did not follow each other successively. Overall, the interaction effects revealed a decrease in task difficulty

with an increase in coherence level within each action class, as reflected in the mean stimulus-locked CPP amplitude.

Table 3.5: Post-Hoc Comparisons for the Interaction of Action Class x Coherence on the Mean Stimulus-Locked CPP Amplitude

| | | Mean Difference | SE | t | $p_{bonf}$ | |
|---|---|---|---|---|---|---|
| Man CL9 | Skin CL9 | -.522 | .231 | -2.259 | 1 | |
| | Loc CL9 | -.704 | .231 | -3.043 | .203 | |
| | Man CL15 | -.373 | .206 | -1.814 | 1 | |
| | Skin CL15 | -.898 | .25 | -3.594 | .032 | * |
| | Loc CL15 | -1.254 | .25 | -5.019 | <.001 | *** |
| | Man CL20 | -.909 | .206 | -4.418 | .001 | ** |
| | Skin CL20 | -1.878 | .25 | -7.519 | <.001 | *** |
| | Loc CL20 | -1.62 | .25 | -6.483 | <.001 | *** |
| | Man CL35 | -1.696 | .206 | -8.245 | <.001 | *** |
| | Skin CL35 | -2.826 | .25 | -11.311 | <.001 | *** |
| | Loc CL35 | -2.032 | .25 | -8.134 | <.001 | *** |
| Skin CL9 | Loc CL9 | -.181 | .231 | -.784 | 1 | |
| | Man CL15 | .149 | .25 | .597 | 1 | |
| | Skin CL15 | -.376 | .206 | -1.825 | 1 | |
| | Loc CL15 | -.732 | .25 | -2.929 | .273 | |
| | Man CL20 | -.387 | .25 | -1.548 | 1 | |
| | Skin CL20 | -1.356 | .206 | -6.591 | <.001 | *** |
| | Loc CL20 | -1.097 | .25 | -4.392 | .002 | ** |
| | Man CL35 | -1.174 | .25 | -4.699 | <.001 | *** |
| | Skin CL35 | -2.303 | .206 | -11.196 | <.001 | *** |
| | Loc CL35 | -1.51 | .25 | -6.044 | <.001 | *** |
| Loc CL9 | Man CL15 | .33 | .25 | 1.322 | 1 | |
| | Skin CL15 | -.194 | .25 | -.778 | 1 | |
| | Loc CL15 | -.55 | .206 | -2.675 | .555 | |
| | Man CL20 | -.205 | .25 | -.822 | 1 | |
| | Skin CL20 | -1.175 | .25 | -4.702 | <.001 | *** |
| | Loc CL20 | -.916 | .206 | -4.452 | .001 | ** |

| | | | | | | |
|---|---|---|---|---|---|---|
| | Man CL35 | -.993 | .25 | -3.974 | .008 | ** |
| | Skin CL35 | -2.122 | .25 | -8.495 | <.001 | *** |
| | Loc CL35 | -1.329 | .206 | -6.458 | <.001 | *** |
| Man CL15 | Skin CL15 | -.525 | .231 | -2.269 | 1 | |
| | Loc CL15 | -.881 | .231 | -3.809 | .017 | * |
| | Man CL20 | -.536 | .206 | -2.604 | .678 | |
| | Skin CL20 | -1.505 | .25 | -6.025 | <.001 | *** |
| | Loc CL20 | -1.246 | .25 | -4.989 | <.001 | *** |
| | Man CL35 | -1.323 | .206 | -6.431 | <.001 | *** |
| | Skin CL35 | -2.452 | .25 | -9.817 | <.001 | *** |
| | Loc CL35 | -1.659 | .25 | -6.641 | <.001 | *** |
| Skin CL15 | Loc CL15 | -.356 | .231 | -1.54 | 1 | |
| | Man CL20 | -.011 | .25 | -.044 | 1 | |
| | Skin CL20 | -.98 | .206 | -4.766 | <.001 | *** |
| | Loc CL20 | -.722 | .25 | -2.889 | .308 | |
| | Man CL35 | -.798 | .25 | -3.196 | .12 | |
| | Skin CL35 | -1.928 | .206 | -9.371 | <.001 | *** |
| | Loc CL35 | -1.134 | .25 | -4.54 | <.001 | *** |
| Loc CL15 | Man CL20 | .345 | .25 | 1.381 | 1 | |
| | Skin CL20 | -.624 | .25 | -2.499 | .92 | |
| | Loc CL20 | -.366 | .206 | -1.777 | 1 | |
| | Man CL35 | -.442 | .25 | -1.771 | 1 | |
| | Skin CL35 | -1.572 | .25 | -6.292 | <.001 | *** |
| | Loc CL35 | -.778 | .206 | -3.782 | .015 | * |
| Man CL20 | Skin CL20 | -.969 | .231 | -4.193 | .004 | ** |
| | Loc CL20 | -.711 | .231 | -3.074 | .185 | |
| | Man CL35 | -.787 | .206 | -3.827 | .013 | * |
| | Skin CL35 | -1.917 | .25 | -7.673 | <.001 | *** |
| | Loc CL35 | -1.123 | .25 | -4.496 | .001 | ** |
| Skin CL20 | Loc CL20 | .259 | .231 | 1.119 | 1 | |
| | Man CL35 | .182 | .25 | .729 | 1 | |
| | Skin CL35 | -.947 | .206 | -4.605 | <.001 | *** |
| | Loc CL35 | -.154 | .25 | -.616 | 1 | |

| | | | | | | |
|---|---|---|---|---|---|---|
| Loc CL20 | Man CL35 | -.077 | .25 | -.307 | 1 | |
| | Skin CL35 | -1.206 | .25 | -4.828 | <.001 | *** |
| | Loc CL35 | -.413 | .206 | -2.005 | 1 | |
| Man CL35 | Skin CL35 | -1.129 | .231 | -4.885 | <.001 | *** |
| | Loc CL35 | -.336 | .231 | -1.453 | 1 | |
| Skin CL35 | Loc CL35 | .794 | .231 | 3.432 | .06 | |

*Note.* P-value adjusted for comparing a family of 66

*Note.* The abbreviations *Man*, *Skin*, *Loc* refer to manipulation actions, skin-displacement actions, and locomotion actions, respectively.

#### 3.2.1.2 Response-Locked Analysis

The response-locked CPP waveforms were expected to reach a common threshold value upon response-execution within each action-class; however this pattern was truly observed only in the CPP signal elicited by the locomotion class stimuli (Figure 3.6).

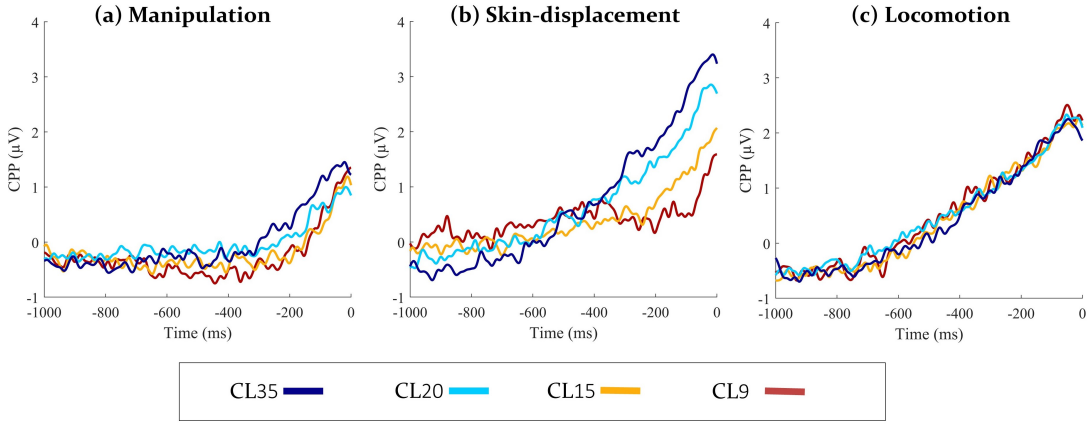


Figure 3.6: Response-Locked Grand-Averaged CPPs Across Action Classes

A 3x4 factorial mass univariate analysis - with factors action class and coherence - of the response-locked ERPs over the centroparietal electrodes indicated the main effects of action class (Figure 3.7) and of coherence levels (Figure 3.8) over the inspected range of the signal.

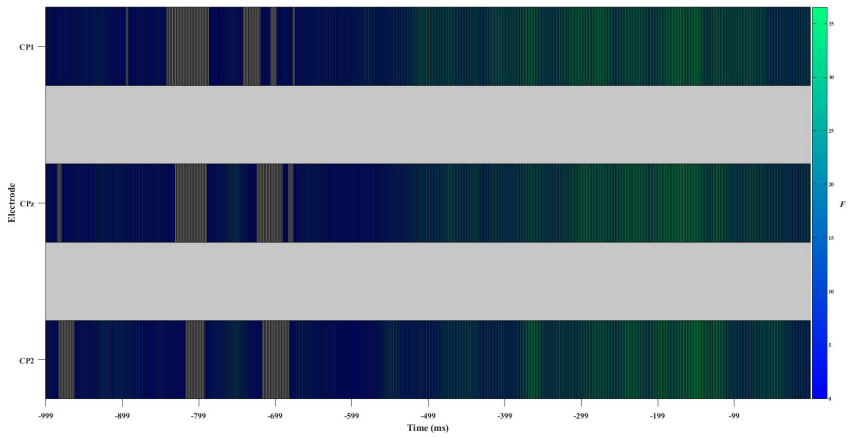


Figure 3.7: Factorial Mass Univariate Analysis of Response-Locked CPP Over Centro Parietal Channels, *Displaying the Main Effect of Action Class*

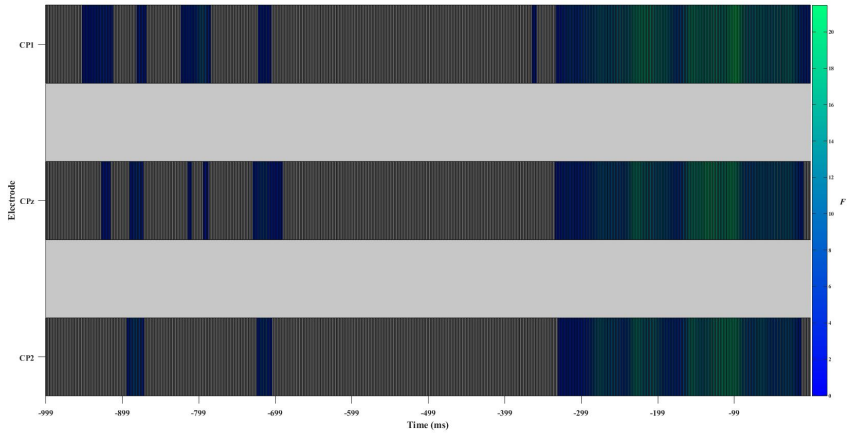


Figure 3.8: Factorial Mass Univariate Analysis of Response-Locked CPP Over Centro Parietal Channels, *Displaying the Main Effect of Coherence*

A 3x4 R-ANOVA on the mean amplitude of the CPP signal over the -300-0ms time interval revealed significant main effects of action class ($F(1.972, 31.556) = 39.997$, $p < .001$, $\eta^2 = .454$) and coherence ($F(2.038, 32.608) = 25.073$, $p < .001$, $\eta^2 = .111$) with a significant interaction between action class and coherence level ($F(3.999, 63.988) = 17.258$, $p < .001$, $\eta^2 = .116$). Follow-up post-hoc comparisons on the action class showed that the mean CPP amplitude was significantly smaller for the manipulation actions ($M = .360$, $SD = .789$) compared to skin-displacement actions ($M = 1.448$, $SD = .957$) and locomotion actions ($M =$

1.650, $SD = .984$), as given in Table 3.6.

Table 3.6: Post-Hoc Comparisons Between the Levels of Action Class on the Mean Response-Locked CPP Amplitude

| | | Mean Difference | SE | t | $p_{bonf}$ | |
|---|---|---|---|---|---|---|
| Man | Skin | -1.088 | .155 | -7.010 | <.001 | *** |
| | Loc | -1.290 | .155 | -8.316 | <.001 | *** |
| Skin | Loc | -.203 | .155 | -1.306 | .603 | |

*Note.* P-value adjusted for comparing a family of 3 estimates

*Note.* Results are averaged over the levels of: *Coherence*

*Note.* The abbreviations *Man*, *Skin*, *Loc* refer to manipulation actions, skin-displacement actions, and locomotion actions, respectively.

Post-hoc comparisons of the coherence levels revealed that in almost all pairs, the condition with the smaller coherence value had a lower mean CPP amplitude compared to the condition with a higher coherence level, albeit the significance of the difference varied between pairs, as presented in Table 3.7.

Table 3.7: Post-Hoc Comparisons Between the Levels of Coherence on the Mean Response-Locked CPP Amplitude

| | | Mean Difference | SE | t | $p_{bonf}$ | |
|---|---|---|---|---|---|---|
| CL9 | CL15 | -.110 | .091 | -1.202 | 1 | |
| | CL20 | -.430 | .091 | -4.713 | <.001 | *** |
| | CL35 | -.714 | .091 | -7.816 | <.001 | *** |
| CL15 | CL20 | -.321 | .091 | -3.511 | .006 | ** |
| | CL35 | -.604 | .091 | -6.613 | <.001 | *** |
| CL20 | CL35 | -.283 | .091 | -3.103 | .019 | * |

*Note.* P-value adjusted for comparing a family of 6

*Note.* Results are averaged over the levels of *Action Class*

Furthermore, the interaction effects (see Table 3.8) revealed a pattern independent of the coherence level on the mean response-locked CPP amplitude, except for the significant differences between the highest coherence level and the two

lowest coherence levels in the manipulation class. Meanwhile, the mean CPP amplitude was significantly elevated in the skin-displacement class with increasing coherence levels. In contrast, the mean CPP amplitude did not differ significantly due to the coherence levels within the locomotion class. Overall, the interaction effects revealed that the mean response-locked CPP amplitude did not differ significantly between coherence levels within manipulation and locomotion action classes, while a significant effect of coherence levels existed in the mean CPP amplitude within the skin-displacement action class.

Table 3.8: Post-Hoc Comparisons for the Interaction of Action Class x Coherence on the Mean Response-Locked CPP Amplitude

| | | Mean Difference | SE | t | $p_{bonf}$ | |
|---|---|---|---|---|---|---|
| Man CL9 | Skin CL9 | -.436 | .181 | -2.405 | 1 | |
| | Loc CL9 | -1.529 | .181 | -8.433 | <.001 | *** |
| | Man CL15 | .026 | .127 | .201 | 1 | |
| | Skin CL15 | -.871 | .193 | -4.509 | .002 | ** |
| | Loc CL15 | -1.449 | .193 | -7.503 | <.001 | *** |
| | Man CL20 | -.179 | .127 | -1.41 | 1 | |
| | Skin CL20 | -1.624 | .193 | -8.41 | <.001 | *** |
| | Loc CL20 | -1.453 | .193 | -7.521 | <.001 | *** |
| | Man CL35 | -.55 | .127 | -4.325 | .002 | ** |
| | Skin CL35 | -2.123 | .193 | -1.99 | <.001 | *** |
| | Loc CL35 | -1.433 | .193 | -7.421 | <.001 | *** |
| Skin CL9 | Loc CL9 | -1.093 | .181 | -6.028 | <.001 | *** |
| | Man CL15 | .462 | .193 | 2.39 | 1 | |
| | Skin CL15 | -.435 | .127 | -3.42 | .056 | |
| | Loc CL15 | -1.013 | .193 | -5.245 | <.001 | *** |
| | Man CL20 | .257 | .193 | 1.329 | 1 | |
| | Skin CL20 | -1.188 | .127 | -9.344 | <.001 | *** |
| | Loc CL20 | -1.017 | .193 | -5.263 | <.001 | *** |
| | Man CL35 | -.114 | .193 | -.59 | 1 | |
| | Skin CL35 | -1.687 | .127 | -13.264 | <.001 | *** |
| | Loc CL35 | -.997 | .193 | -5.164 | <.001 | *** |

| | | | | | | |
|---|---|---|---|---|---|---|
| Loc CL9 | Man CL15 | 1.555 | .193 | 8.05 | <.001 | *** |
| | Skin CL15 | .658 | .193 | 3.408 | .072 | |
| | Loc CL15 | .08 | .127 | .63 | 1 | |
| | Man CL20 | 1.35 | .193 | 6.989 | <.001 | *** |
| | Skin CL20 | -.095 | .193 | -.492 | 1 | |
| | Loc CL20 | .077 | .127 | .603 | 1 | |
| | Man CL35 | .979 | .193 | 5.07 | <.001 | *** |
| | Skin CL35 | -.593 | .193 | -3.073 | .199 | |
| | Loc CL35 | .096 | .127 | .754 | 1 | |
| Man CL15 | Skin CL15 | -.897 | .181 | -4.944 | <.001 | *** |
| | Loc CL15 | -1.475 | .181 | -8.132 | <.001 | *** |
| | Man CL20 | -.205 | .127 | -1.611 | 1 | |
| | Skin CL20 | -1.65 | .193 | -8.542 | <.001 | *** |
| | Loc CL20 | -1.478 | .193 | -7.653 | <.001 | *** |
| | Man CL35 | -.575 | .127 | -4.525 | <.001 | *** |
| | Skin CL35 | -2.148 | .193 | -11.122 | <.001 | *** |
| | Loc CL35 | -1.459 | .193 | -7.553 | <.001 | *** |
| Skin CL15 | Loc CL15 | -.578 | .181 | -3.188 | .153 | |
| | Man CL20 | .692 | .193 | 3.581 | .041 | * |
| | Skin CL20 | -.753 | .127 | -5.924 | <.001 | *** |
| | Loc CL20 | -.582 | .193 | -3.012 | .238 | |
| | Man CL35 | .321 | .193 | 1.662 | 1 | |
| | Skin CL35 | -1.252 | .127 | -9.844 | <.001 | *** |
| | Loc CL35 | -.562 | .193 | -2.912 | .317 | |
| Loc CL15 | Man CL20 | 1.27 | .193 | 6.575 | <.001 | *** |
| | Skin CL20 | -.175 | .193 | -.907 | 1 | |
| | Loc CL20 | -.003 | .127 | -.027 | 1 | |
| | Man CL35 | .899 | .193 | 4.656 | <.001 | *** |
| | Skin CL35 | -.674 | .193 | -3.487 | .056 | |
| | Loc CL35 | .016 | .127 | .124 | 1 | |
| Man CL20 | Skin CL20 | -1.445 | .181 | -7.968 | <.001 | *** |
| | Loc CL20 | -1.273 | .181 | -7.022 | <.001 | *** |
| | Man CL35 | -.371 | .127 | -2.915 | .278 | |

| | | | | | | |
|---|---|---|---|---|---|---|
| | Skin CL35 | -1.944 | .193 | -1.062 | <.001 | *** |
| | Loc CL35 | -1.254 | .193 | -6.493 | <.001 | *** |
| Skin CL20 | Loc CL20 | .172 | .181 | .946 | 1 | |
| | Man CL35 | 1.074 | .193 | 5.562 | <.001 | *** |
| | Skin CL35 | -.498 | .127 | -3.92 | .010 | ** |
| | Loc CL35 | .191 | .193 | .988 | 1 | |
| Loc CL20 | Man CL35 | .903 | .193 | 4.674 | <.001 | *** |
| | Skin CL35 | -.67 | .193 | -3.469 | .059 | |
| | Loc CL35 | .019 | .127 | .151 | 1 | |
| Man CL35 | Skin CL35 | -1.573 | .181 | -8.673 | <.001 | *** |
| | Loc CL35 | -.883 | .181 | -4.872 | <.001 | *** |
| Skin CL35 | Loc CL35 | .689 | .181 | 3.801 | .023 | * |

*Note.* P-value adjusted for comparing a family of 66

*Note.* The abbreviations *Man*, *Skin*, *Loc* refer to manipulation actions, skin-displacement actions, and locomotion actions, respectively.

### 3.2.2 Lateralized Readiness Potential

The visual inspection of both the stimulus-locked (Figure 3.9) and response-locked (Figure 3.10) LRP signals did not indicate differences between conditions; an FDR-corrected mass-univariate approach that was employed to investigate the existence of an effect yielded no significant differences between any time points in any condition ($p > .05$).

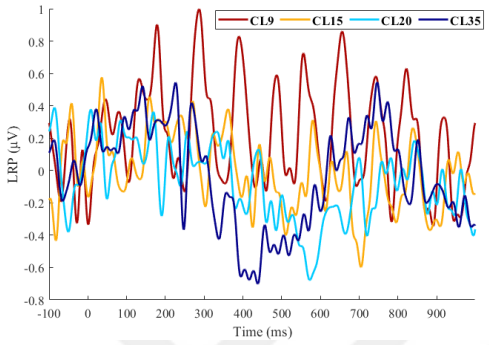


(a) Manipulation C3/C4 pair

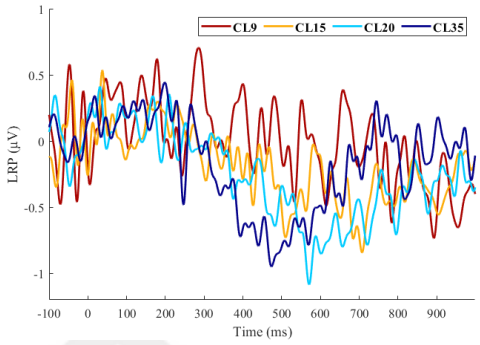


(b) Manipulation FC3/FC4 pair

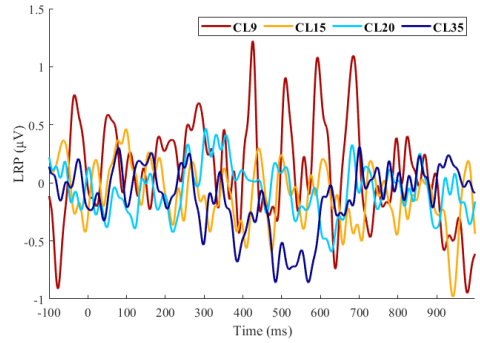


(c) Skin-Displacement C3/C4 pair

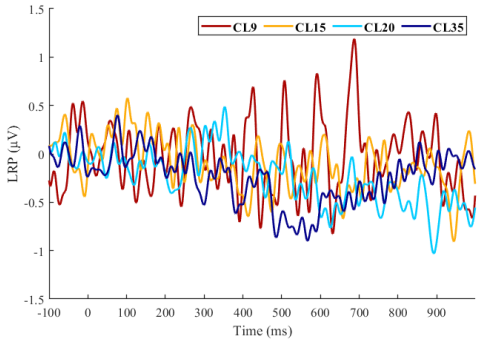


(d) Skin-Displacement FC3/FC4 pair

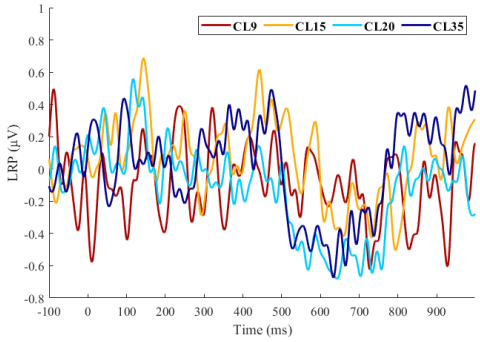


(e) Locomotion C3/C4 pair

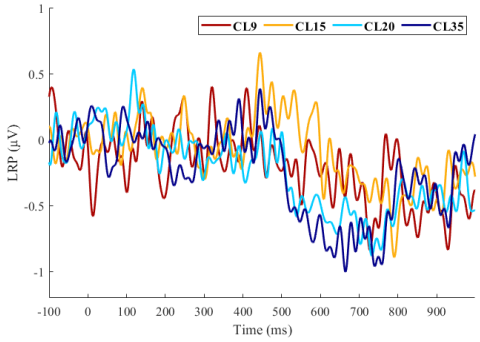


(f) Locomotion FC3/FC4 pair

Figure 3.9: Stimulus-Locked Grand-Averaged LRPs Across Action Classes

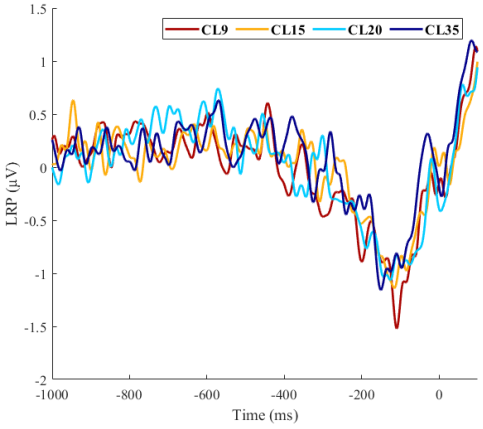


(a) Manipulation C3/C4 pair

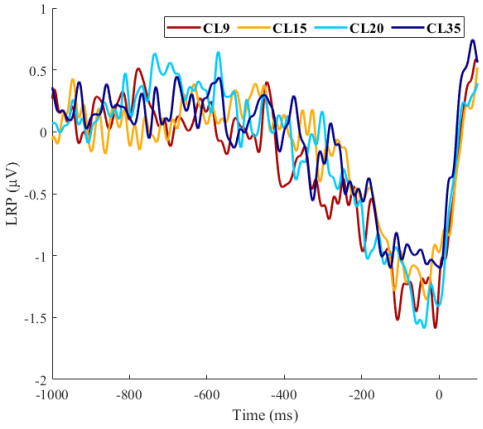


(b) Manipulation FC3/FC4 pair

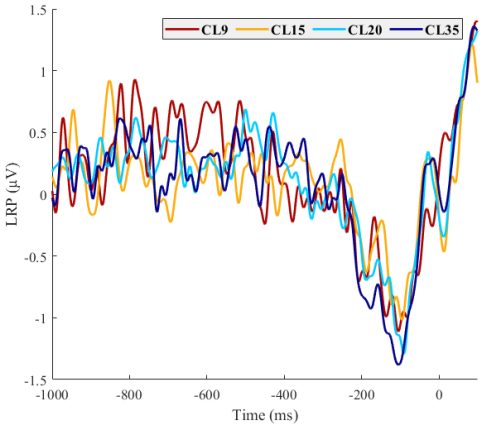


(c) Skin-Displacement C3/C4 pair

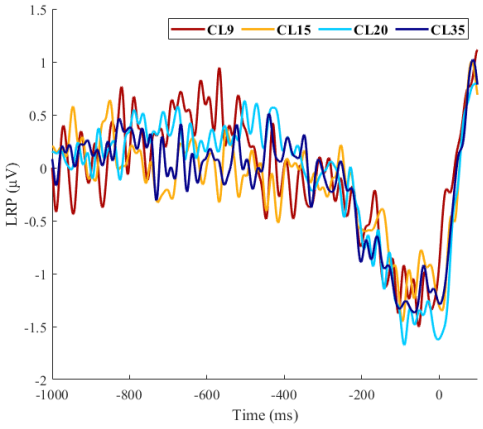


(d) Skin-Displacement FC3/FC4 pair

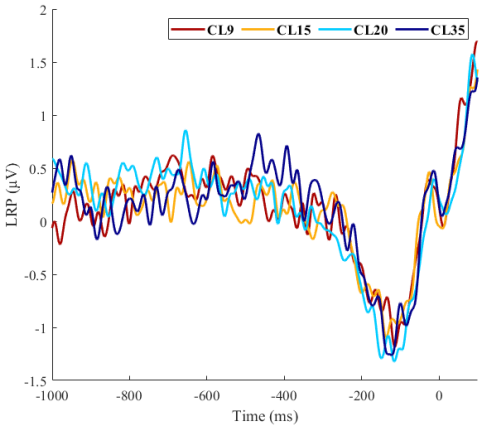


(e) Locomotion C3/C4 pair

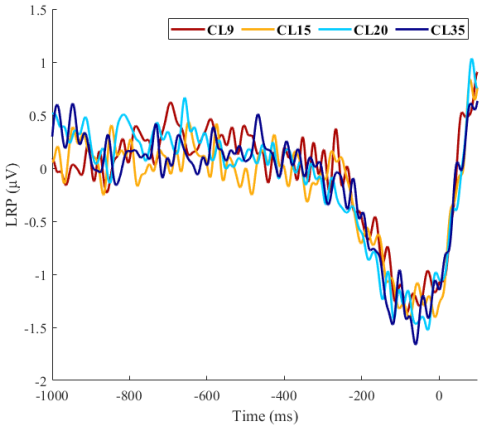


(f) Locomotion FC3/FC4 pair

Figure 3.10: Response-Locked Grand-Averaged LRPs Across Action Classes

# Chapter 4

# Discussion

The current study investigated the neural basis of naturalistic action perception during a perceptual decision-making task separately for three action classes. The task difficulty is primarily controlled by manipulating coherence levels within each action discrimination task. The success of the manipulation is justified by the significant differences between coherence levels in behavioral metrics; both mean response time and percentage miss rate decayed with increasing sensory information. The impact of coherence was further elaborated by the build-to-threshold dynamics of the stimulus-aligned CPP during the evidence accumulation stage, which showed elevated peak values and higher mean amplitudes for higher coherence levels compared to lower levels, thereby displaying the first feature of a decision variable. Together with the coherence, the action class appeared to have significant effects on behavioral and neural metrics. On the other hand, the response-aligned CPPs within action classes successfully demonstrated the sensory independent characteristics of a decision variable, except for the skin-displacement class. Meanwhile, the LRP signal exhibited pure motor characteristics in both stimulus and response-aligned traces.

In this section, the main findings of this study will be explained by grouping them according to the two stages of the decision-making processes: decision formation and motor response planning/execution.

## 4.1 Decision Formation is Mirrored by the Centro Parietal Positivity

The formation of a decision involves the integration of sensory evidence into a decision variable to finalize the decision process when it passes a threshold. In the scope of this study, the decision-formation stage reflected by the CPP was hypothesized to be impacted both by the differences in the levels of coherence and the identity of actions, and the stimulus-locked CPP results confirmed this hypothesis.

Considering the data for each action task separately, the results display the existence of a robust CPP that is notably affected by the strength of sensory information. Such an observation of the CPP signal is in accordance with the findings of the previous studies that investigated the same stage by employing the perception of different stimulus sets in discrimination tasks either by tracking CPP in humans [26, 27, 30, 32, 34] or tracking single neurons in non-human primates [14, 15, 16]. To the best of our knowledge, this is the first study that investigated the ERP correlates of natural action perception in an action discrimination scenario. The fact that CPP also showed the same properties in a discrimination experiment requiring the perception of natural action movements demonstrated the generalizability of this signal to ecologically valid and complex stimuli perception.

An investigation of the stimulus-aligned CPP across action classes revealed intriguing differences. First, the visual inspection of the time courses of three CPP signals revealed that the starting moment of build-up was approximately the same across the three actions (around 200 ms), which disproved our hypothesis on the latency of the CPPs for natural action perception. Contrary to our expectations, CPPs following the natural motion discrimination process started to rise earlier than in the biological motion perception study [34]. We predict that the reason for this earlier onset latency may be arising due to the difference in the strength of form information in biological motion stimulus and natural action stimulus. Compared to natural action, biological motion stimuli generated by PLDs have

a much weaker form of information. Hence, the elevated strength of the form feature may have accelerated the stages of decision-making for natural actions.

Despite sharing approximately the same moment of build-up, it took longer for the CPP elicited in the locomotion class to reach its peak amplitude compared to the other two. Even though the significance of this difference has not been statistically tested, the reason for this slow rate of build-up may have appeared due to the evolutionary importance of the locomotion actions compared to two other actions. Considering the significantly elevated bound parameter for the locomotion exemplars reported by Platonov and Orban [49], the slower build-up in the CPPs of locomotion actions might be reflecting a slowly growing decision variable to reach a higher bound as in line with the implications of diffusion models [5, 6, 54].

Secondly, the mean amplitude of CPPs in the manipulation class was found to be significantly lower than in the other classes, and this difference was also visible in the peak amplitudes of the CPPs when all action classes were examined separately at each level of coherence. Additionally, even though the miss rate scores did not significantly differ between manipulation and locomotion actions with near-perfect performances, the mean response time for the discrimination of manipulation actions was significantly lower than for locomotion actions. Collectively, these results and observations support the findings of the study that obtained significantly higher bound parameters for locomotion class compared to manipulation [49] since, from a theoretical framework, a decision variable reaches a lower bound faster compared to a higher bound [8].

Overall, the stimulus-locked CPPs within and across action classes displayed the characteristics of a true decision variable growing in accordance with the incoming sensory evidence. The impacts of coherence and action class were visible from the time course of the evolving decision variable, and statistical reports supported their effects. The presence of the effects of action classes during the decision-formation stage supported the notion that the perception of observed actions is affiliated with the encoding of the sensory information stage within a decision-making process [44].

## 4.2 Response-Locked Centro Parietal Positivity Might Reflect Task Difficulty

The second feature of a classical decision variable is that it converges to a stereotypical threshold value just before a response is initiated, regardless of the difficulty of the task. In line with this, the response-aligned CPPs following the coherence levels within each action class were hypothesized to reach a common voltage level before response execution.

In contrary to that hypothesis, the response-aligned CPPs displayed differing patterns within and across action classes. One outstanding difference was observed between the response-locked CPPs of locomotion actions, where the CPPs representing each level of coherence are almost identical, and skin-displacement actions, where the CPPs seem to follow the coherence levels. One possible explanation for this outcome is that the size of the areas encompassing the movement trajectories of the limbs performing the actions can increase or decrease the effect of the applied coherence manipulation. The validity of this interpretation for this study is supported by the percent miss-rate results, which deviate significantly from perfect performance for the skin-displacement class while indicating near-perfect performance in the locomotion and manipulation classes. In addition, based on the studies that identified the areas showing selectivity in PPC for the three action classes of interest [45, 46, 47], the smallest area belongs to skin-displacement actions while the largest area shows selectivity towards observing locomotion actions. In accordance with the interpretations of Platonov and Orban [49], the size of the selectively activated neurons might boost the discrimination performance of observed action exemplars. Finally, several recent studies have observed the amplitude of the response-locked CPP to be affected by the difficulty of the task [55, 56], further supporting our interpretation of this incongruity between action classes.

While response-locked analysis of the CPP carried the effects of both manipulations of the stimulus (action class and coherence) in both its visual trace and in its mean amplitude, response-locked analysis of all combinations of the LRP

signal, both within and between action classes, converged to common threshold levels with no significant differences at any time point during the time course. Therefore, as hypothesized, the LRP showed purely motor dynamics that are independent of the sensory evidence.

Overall, the response-aligned analyses of ERPs of interest revealed that LRP and CPP differed in terms of their dependence on the manipulations of sensory information. Even though LRPs exhibited robust independence from the stages other than motor planning and execution, the CPPs were significantly impacted by the factors important for the encoding and perception of the natural actions.

## 4.3 Limitations and Future Work

While providing the first concrete evidence for the generalization of the functional properties of the CPP signal as a decision variable to the decision processes involving natural action perception and how several defining parameters change in accordance with the action category, our study comes with a couple of limitations.

The first limitation occurs due to the uneven manipulation of the signal-to-noise ratio between the stimuli from different action classes. Even though we have applied the same fixed parameters for generating noise for each action class, due to the nature of actions and the size of the area in which the action is being executed, the same coherence levels did not result in exactly the same difficulties. For example, a locomotion exemplar of this study constituted a larger area in the visual field since such an action is executed using the full body (both arms and legs); however, a skin-displacement exemplar constituted a much smaller area since it mainly covered an area that is in size of a palm. The existence of unequal noise levels might be one of the leading causes that yielded higher miss-rates for the lowest coherence condition in the skin-displacement actions. Thereby, a fruitful future direction could be to equate the perceived difficulties of the coherence levels across action classes to validate the findings of this study.

The second limitation, which may have induced a bias in the perceived difficulty of experimental sessions, is the existence of three behavioral sessions prior to the EEG experiments. According to the verbal reports of the participants after behavioral parts, the manipulation sessions were regarded as the *easiest*, whereas the skin-displacement sessions were classified as the *hardest* discrimination tasks. The back-to-back participation in the behavioral sessions might have led to the generation of a bias towards a specific action class. Therefore, future work could approach this limitation by implementing a between-subject design to at least prevent participants from comparing the difficulties between action classes, which would prevent unwanted biases.

Lastly, in the scope of this study, the fact that the neural traces of decision-making processes were studied using scalp EEG can be seen as a limitation. The reason for this is that it is quite difficult for signals that are not very strongly elicited or are represented with less activity to preserve their effects all the way to the scalp. Our results also reveal that the locomotion class, which has a wider representation area compared to manipulation and skin-displacement actions, has higher amplitudes, especially at low coherence levels. For this reason, if future studies investigate these discrimination tasks using intracranial EEG, it might show how well our findings obtained with scalp EEG can probe the effects of action classes.

## 4.4 Conclusion

In conclusion, this study investigated the neural basis of the perception of natural actions within the framework of perceptual decision-making using three separate action discrimination tasks. Within each task, the task difficulty was primarily controlled by coherence levels, albeit the identity of the actions has also been found to contribute to the perceived difficulty. The trends in mean response time and percent miss rate reflected the significance of the manipulations in the coherence and action class. The stimulus-locked CPP showed clear features of a robust evolving decision variable tracking the coherence level within each action

class experiment. In contrast, during the same time course, LRP showed no trace that could be related to evidence accumulation. The analysis of the CPP and LRP aligned to the response revealed differences among action classes and coherence levels among CPP, though the LRP manifested the features of a purely motor signal. Altogether, our findings are broadly in line with previous literature and are the first to demonstrate that decision processes described using simpler or artificial stimuli are also valid for discrimination decisions that require the perception of natural actions.

# References


[1] R. Ratcliff, P. L. Smith, S. D. Brown, and G. McKoon, "Diffusion decision model: Current issues and history," *Trends in Cognitive Sciences*, vol. 20, no. 4, pp. 260–281, 2016.

[2] D. Gilles and R. Jörg, "Comparing perceptual and preferential decision making," *Psychonomic Bulletin & Review*, vol. 23, pp. 723–737, 2016.

[3] F. C. Donders, "On the speed of mental processes," *Acta Psychologica*, vol. 30, pp. 412–431, 1969.

[4] R. A. Abrams and D. A. Balota, "Mental chronometry: Beyond reaction time," *Psychological Science*, vol. 2, no. 3, pp. 153–157, 1991.

[5] R. Ratcliff and G. McKoon, "The diffusion decision model: Theory and data for two-choice decision tasks," *Neural Computation*, vol. 20, no. 4, pp. 873–922, 2008.

[6] C. E. Myers, A. Interian, and A. A. Moustafa, "A practical introduction to using the drift diffusion model of decision-making in cognitive psychology, neuroscience, and health sciences," *Frontiers in Psychology*, vol. 13, p. 1039172, 2022.

[7] J. Vandekerckhove and F. Tuerlinckx, "Fitting the ratcliff diffusion model to experimental data," *Psychonomic Bulletin & Review*, vol. 14, pp. 1011–1026, 2007.

[8] R. Ratcliff and J. N. Rouder, "Modeling response times for two-choice decisions," *Psychological Science*, vol. 9, no. 5, pp. 347–356, 1998.

[9] J. Palmer, A. C. Huk, and M. N. Shadlen, "The effect of stimulus strength on the speed and accuracy of a perceptual decision," *Journal of Vision*, vol. 5, pp. 1–1, 5 2005.

[10] M. J. Mulder, E. J. Wagenmakers, R. Ratcliff, W. Boekel, and B. U. Forstmann, "Bias in the brain: A diffusion model analysis of prior probability and potential payoff," *Journal of Neuroscience*, vol. 32, no. 7, pp. 2335–2343, 2012.

[11] J. I. Gold and M. N. Shadlen, "The neural basis of decision making," *Annual Review of Neuroscience*, vol. 30, pp. 535–574, 2007.

[12] H. R. Heekeren, S. Marrett, and L. G. Ungerleider, "The neural systems that mediate human perceptual decision making," *Nature reviews. Neuroscience*, vol. 9, pp. 467–479, 2008.

[13] C. D. Salzman, C. M. Murasugi, K. H. Britten, and W. T. Newsome, "Microstimulation in visual area mt: Effects on direction discrimination performance," *Journal of Neuroscience*, vol. 12, no. 6, pp. 2331–2355, 1992.

[14] M. N. Shadlen and W. T. Newsome, "Motion perception: Seeing and deciding.," *Proceedings of the National Academy of Sciences*, vol. 93, no. 2, pp. 628–633, 1996.

[15] J. N. Kim and M. N. Shadlen, "Neural correlates of a decision in the dorsolateral prefrontal cortex of the macaque," *Nature Neuroscience*, vol. 2, no. 2, pp. 176–185, 1999.

[16] M. N. Shadlen and W. T. Newsome, "Neural basis of a perceptual decision in the parietal cortex (area lip) of the rhesus monkey," *Journal of Neurophysiology*, vol. 86, no. 4, pp. 1916–1936, 2001.

[17] J. D. Roitman and M. N. Shadlen, "Response of neurons in the lateral intraparietal area during a combined visual discrimination reaction time task," *Journal of Neuroscience*, vol. 22, no. 21, pp. 9475–9489, 2002.

[18] R. Kiani and M. N. Shadlen, "Representation of confidence associated with a decision by neurons in the parietal cortex," *Science*, vol. 324, no. 5928, pp. 759–764, 2009.

[19] K. H. Britten, M. N. Shadlen, W. T. Newsome, and J. A. Movshon, "The analysis of visual motion: A comparison of neuronal and psychophysical performance," *Journal of Neuroscience*, vol. 12, no. 12, pp. 4745–4765, 1992.

[20] W. T. Newsome and E. B. Pare, "A selective impairment of motion perception following lesions of the middle temporal visual area (mt)," *Journal of Neuroscience*, vol. 8, no. 6, pp. 2201–2211, 1988.

[21] D. L. Sparks, "Translation of sensory signals into commands for control of saccadic eye movements: Role of primate superior colliculus," *Physiological Reviews*, vol. 66, no. 1, pp. 118–171, 1986.

[22] J. D. Schall, "On the role of frontal eye field in guiding attention and saccades," *Vision Research*, vol. 44, no. 12, pp. 1453–1467, 2004.

[23] S. P. Kelly and R. G. O'Connell, "The neural processes underlying perceptual decision making in humans: Recent progress and future directions," *Journal of Physiology, Paris*, vol. 109, no. 1-3, pp. 27–37, 2015.

[24] T. D. Hanks and C. Summerfield, "Perceptual decision making in rodents, monkeys, and humans," *Neuron*, vol. 93, no. 1, pp. 15–31, 2017.

[25] C. Summerfield and A. Blangero, "Perceptual decision-making: What do we know, and what do we not know?," in *Decision Neuroscience*, pp. 149–162, Academic Press, 2017.

[26] R. G. O'Connell, P. M. Dockree, and S. P. Kelly, "A supramodal accumulation-to-bound signal that determines perceptual decisions in humans," *Nature Neuroscience*, vol. 15, no. 12, pp. 1729–1735, 2012.

[27] S. P. Kelly and R. G. O'Connell, "Internal and external influences on the rate of sensory evidence accumulation in the human brain," *Journal of Neuroscience*, vol. 33, no. 50, pp. 19434–19441, 2013.

[28] R. de Jong, M. Wierda, G. Mulder, and L. J. Mulder, "Use of partial stimulus information in response processing.," *Journal of Experimental Psychology: Human Perception and Performance*, vol. 14, no. 4, pp. 682–692, 1988.

[29] J. Herding, S. Ludwig, A. von Lautz, B. Spitzer, and F. Blankenburg, "Centro-parietal eeg potentials index subjective evidence and confidence during perceptual decision making," *NeuroImage*, vol. 201, p. 116011, 2019.

[30] M. K. van Vugt, M. A. Beulen, and N. A. Taatgen, "Relation between centro-parietal positivity and diffusion model parameters in both perceptual and memory-based decision making," *Brain Research*, vol. 1715, pp. 1–12, 2019.

[31] N. A. Steinemann, R. G. O'Connell, and S. P. Kelly, "Decisions are expedited through multiple neural adjustments spanning the sensorimotor hierarchy," *Nature Communications*, vol. 9, no. 1, p. 3627, 2018.

[32] S. P. Kelly, E. A. Corbett, and R. G. O'Connell, "Neurocomputational mechanisms of prior-informed perceptual decision-making in humans," *Nature Human Behaviour*, vol. 5, no. 4, pp. 467–481, 2021.

[33] C. F. Tagliabue, D. Veniero, C. S. Y. Benwell, R. Cecere, S. Savazzi, and G. Thut, "The eeg signature of sensory evidence accumulation during decision formation closely tracks subjective perceptual experience," *Scientific Reports*, vol. 9, no. 1, p. 4949, 2019.

[34] O. C. Oguz, B. Aydin, and B. A. Urgen, "Biological motion perception in the theoretical framework of perceptual decision-making: An event-related potential study," *Vision Research*, vol. 218, p. 108380, 2024.

[35] G. Johansson, "Visual perception of biological motion and a model for its analysis," *Perception & Psychophysics*, vol. 14, pp. 201–211, 1973.

[36] M. Mishkin, L. G. Ungerleider, and K. A. Macko, "Object vision and spatial vision: Two cortical pathways," *Trends in Neurosciences*, vol. 6, pp. 414–417, 1983.

[37] J. Thompson and R. Parasuraman, "Attention, biological motion, and action recognition," *Neuroimage*, vol. 59, no. 1, pp. 4–13, 2012.

[38] K. J. Wheaton, J. C. Thompson, A. Syngeniotis, D. F. Abbott, and A. Puce, "Viewing the motion of human body parts activates different regions of premotor, temporal, and parietal cortex," *NeuroImage*, vol. 22, no. 1, pp. 277–288, 2004.

[39] G. Buccino, F. Binkofski, G. R. Fink, L. Fadiga, L. Fogassi, V. Gallese, R. J. Seitz, K. Zilles, G. Rizzolatti, and H. J. Freund, "Action observation activates premotor and parietal areas in a somatotopic manner: An fmri study," *European Journal of Neuroscience*, vol. 13, no. 2, pp. 400–404, 2001.

[40] J. Jastorff, C. Begliomini, M. Fabbri-Destro, G. Rizzolatti, and G. A. Orban, "Coding observed motor acts: Different organizational principles in the parietal and premotor cortex of humans," *Journal of Neurophysiology*, vol. 104, no. 1, pp. 128–140, 2010.

[41] A. F. de C. Hamilton and S. T. Grafton, "Action outcomes are represented in human inferior frontoparietal cortex," *Cerebral Cortex*, vol. 18, no. 5, pp. 1160–1168, 2008.

[42] A. F. de C. Hamilton and S. T. Grafton, "Goal representation in human anterior intraparietal sulcus," *Journal of Neuroscience*, vol. 26, no. 4, pp. 1133–1137, 2006.

[43] S. H. Johnson-Frey, F. R. Maloof, R. Newman-Norlund, C. Farrer, S. Inati, and S. T. Grafton, "Actions or hand-object interactions? human inferior frontal cortex and action observation," *Neuron*, vol. 39, no. 6, pp. 1053–1058, 2003.

[44] G. A. Orban, "Action observation as a visual process: Different classes of actions engage distinct regions of human ppc," in *Cultural Patterns and Neurocognitive Circuits II*, pp. 1–32, World Scientific, 2018.

[45] R. O. Abdollahi, J. Jastorff, and G. A. Orban, "Common and segregated processing of observed actions in human spl," *Cerebral Cortex*, vol. 23, no. 11, pp. 2734–2753, 2013.

[46] D. Corbo and G. A. Orban, "Observing others speak or sing activates spt and neighboring parietal cortex," *Journal of Cognitive Neuroscience*, vol. 29, no. 6, pp. 1002–1021, 2017.

[47] S. Ferri, G. Rizzolatti, and G. A. Orban, "The organization of the posterior parietal cortex devoted to upper limb actions: An fmri study," *Human Brain Mapping*, vol. 36, no. 10, pp. 3845–3866, 2015.

[48] A. Platonov and G. A. Orban, "Action observation: The less-explored part of higher-order vision," *Scientific Reports*, vol. 6, no. 1, p. 36742, 2016.

[49] A. Platonov and G. A. Orban, "Not all observed actions are perceived equally," *Scientific Reports*, vol. 7, no. 1, p. 17084, 2017.

[50] The MathWorks Inc., "MATLAB Version R2021b," 2021.

[51] V. Willenbockel, J. Sadr, D. Fiset, G. O. Horne, F. Gosselin, and J. W. Tanaka, "Controlling low-level image properties: The shine toolbox," *Behavior Research Methods*, vol. 42, pp. 671–684, 2010.

[52] A. Delorme and S. Makeig, "Eeglab: An open source toolbox for analysis of single-trial eeg dynamics including independent component analysis," *Journal of Neuroscience Methods*, vol. 134, no. 1, pp. 9–21, 2004.

[53] J. Lopez-Calderon and S. J. Luck, "Erplab: An open-source toolbox for the analysis of event-related potentials," *Frontiers in Human Neuroscience*, vol. 8, p. 213, 2014.

[54] B. U. Forstmann, R. Ratcliff, and E.-J. Wagenmakers, "Sequential sampling models in cognitive neuroscience: Advantages, applications, and extensions," *Annual Review of Psychology*, vol. 67, pp. 641–666, 2016.

[55] L. Spieser, C. Kohl, B. Forster, S. Bestmann, and K. Yarrow, "Neurodynamic evidence supports a forced-excursion model of decision-making under speed/accuracy instructions," *Eneuro*, vol. 5, no. 3, 2018.

[56] C. Kohl, L. Spieser, B. Forster, S. Bestmann, and K. Yarrow, "Centroparietal activity mirrors the decision variable when tracking biased and time-varying sensory evidence," *Cognitive Psychology*, vol. 122, p. 101321, 2020.